metals

Review

A Review of Deformation Mechanisms, Compositional Design, and Development of Titanium Alloys with Transformation-Induced Plasticity and Twinning-Induced Plasticity Effects

Yu Fu [1,2], Yue Gao [1], Wentao Jiang [1], Wenlong Xiao [1,*], Xinqing Zhao [1] and Chaoli Ma [1,3]

[1] Key Laboratory of Aerospace Advanced Materials and Performance of Ministry of Education, School of Materials Science and Engineering, Beihang University, Beijing 100191, China; fuyu@scu.edu.cn (Y.F.); by2101208@buaa.edu.cn (Y.G.); zb2201102@buaa.edu.cn (W.J.); xinqing@buaa.edu.cn (X.Z.); machaoli@buaa.edu.cn (C.M.)
[2] School of Mechanical Engineering, Sichuan University, Chengdu 610065, China
[3] Tianmushan Laboratory, Yuhang District, Hangzhou 311115, China
* Correspondence: wlxiao@buaa.edu.cn

Abstract: Metastable β-type Ti alloys that undergo stress-induced martensitic transformation and/or deformation twinning mechanisms have the potential to simultaneously enhance strength and ductility through the transformation-induced plasticity effect (TRIP) and twinning-induced plasticity (TWIP) effect. These TRIP/TWIP Ti alloys represent a new generation of strain hardenable Ti alloys, holding great promise for structural applications. Nonetheless, the relatively low yield strength is the main factor limiting the practical applications of TRIP/TWIP Ti alloys. The intricate interplay among chemical compositions, deformation mechanisms, and mechanical properties in TRIP/TWIP Ti alloys poses a challenge for the development of new TRIP/TWIP Ti alloys. This review delves into the understanding of deformation mechanisms and strain hardening behavior of TRIP/TWIP Ti alloys and summarizes the role of β phase stability, α″ martensite, α′ martensite, and ω phase on the TRIP/TWIP effects. This is followed by the introduction of compositional design strategies that empower the precise design of new TRIP/TWIP Ti alloys through multi-element alloying. Then, the recent development of TRIP/TWIP Ti alloys and the strengthening strategies to enhance their yield strength while preserving high-strain hardening capability are summarized. Finally, future prospects and suggestions for the continued design and development of high-performance TRIP/TWIP Ti alloys are highlighted.

Keywords: titanium alloys; stress-induced martensitic transformation; deformation twinning; deformation mechanism; composition design; yield strength

Citation: Fu, Y.; Gao, Y.; Jiang, W.; Xiao, W.; Zhao, X.; Ma, C. A Review of Deformation Mechanisms, Compositional Design, and Development of Titanium Alloys with Transformation-Induced Plasticity and Twinning-Induced Plasticity Effects. *Metals* **2024**, *14*, 97. https://doi.org/10.3390/met14010097

Academic Editor: Maciej Motyka

Received: 26 October 2023
Revised: 5 January 2024
Accepted: 10 January 2024
Published: 13 January 2024

1. Introduction

The utilization of Ti alloys as high-strength components, such as landing gears, calls for high-strength metastable β-Ti alloys with strength exceeding 1200 MPa. This level of strength is primarily attained through α precipitation strengthening and solid solution strengthening mechanisms [1–3]. However, the successful development of high-strength Ti alloys inevitably comes at the cost of decreased ductility and strain hardening capability owing to the restricted dislocation activity, which is typically faced in the materials' development. For example, the 0.2% yield strength of the most widely used Ti-6Al-4V (weight percentage hereafter unless otherwise specified) can be as high as ~1000 MPa, but its fracture elongation is only 12%, and its strain hardening rate is rather limited [4]. In comparison, a high ductility of 35% and high strain hardening ability (ultimate tensile strength minus yield strength) of about 730 MPa were obtained in a TRIP/TWIP Ti-8Cr-1.5Sn alloy [4]. In addition to high strength, especially the high yield strength required to prevent the alloy from plastic yielding during stress loading, combined high ductility and

high strain hardening are also crucial for Ti alloys to increase the absorbable work before abrupt material fracture, thereby improving the overall service reliability [5].

A feasible way to mitigate the low ductility and limited work hardening observed in high-strength Ti alloys is to introduce additional deformation modes that can accommodate the plastic strain during dynamic deformation. These deformation mechanisms include stress-induced martensite transformation and deformation twinning, which can be achieved by tailoring the phase stability of the body-centered cubic β phase [6–8]. As historically observed in steels, the dynamic phase transformation and twinning during deformation lead to simultaneous improvement in strength, ductility, and strain hardening, a mechanism known as the transformation-induced plasticity (TRIP) effect and twinning-induced plasticity (TWIP) effect [9–11].

Since the first report of Ti-12Mo alloy combining TRIP and TWIP effects in 2012 [12], TRIP/TWIP Ti alloys have attracted increasing interest in the field of Ti science. They constitute an important class of Ti alloy due to their ability to achieve an outstanding combination of high strength, high ductility, and high strain hardening capability. Ongoing efforts are dedicated to designing new TRIP/TWIP Ti alloys with improved yield strength, ultimate tensile strength, and total elongation by manipulating the activation sequence of the various deformation modes [4,8,13–15]. Understanding the intrinsic correlation between the compositional design strategy (specifically, β phase stability), deformation mechanisms, and mechanical properties is essential for the design and development of new TRIP/TWIP Ti alloys that can simultaneously offer high yield strength, high strain hardening capability, and high ductility to meet the ever-growing demands for high-strength Ti alloy in advanced structural applications.

This paper first briefly reviews the deformation mechanisms of the TRIP/TWIP Ti alloy, focusing on the strain hardening behavior associated with the dynamic stress-induced martensitic transformation and mechanical twinning during deformation. We also examine the role of the β phase stability, α″, α′, and ω phases on the deformation mechanism and corresponding mechanical properties of TRIP/TWIP Ti alloys. Subsequently, the compositional design strategies of new alloys within this class based on the semi-empirical methods to tailor the β phase stability and deformation modes are summarized. Finally, we provide a historical perspective on the development of TRIP/TWIP Ti alloys with a particular focus on enhancing the yield strength, aiming to provide valuable insights into improving the overall mechanical properties of TRIP/TWIP Ti alloys.

2. Deformation Mechanisms of TRIP/TWIP Ti Alloys

The merits of TRIP/TWIP Ti alloys predominately stem from the dynamic restriction of dislocation motion during deformation by the various phase interfaces and twin boundaries through a mechanism known as the dynamic Hall–Petch effect. Several factors, such as the β phase stability (chemical composition of the β phase) [16] and the presence of additional phases like α, O′, and ω [15,17–19], play crucial roles in initiating stress-induced phase transformation and deformation twinning, thus the strain hardening capability and mechanical properties of TRIP/TWIP Ti alloys.

2.1. Deformation Mechanisms and Strain Hardening Behavior

Different deformation modes, such as stress-induced phase transformation (including stress-induced body-centered cubic (bcc) β-to-hexagonal close-packed (hcp) α′ martensitic transformation [8,19–22], stress-induced β-to-orthorhombic α″ martensitic transformation [23–27], and stress-induced β-to-ω phase transformation [28–31]), deformation twinning [7,13,14,32–34], and dislocation slipping [35,36], can be activated in Ti alloys accommodating increased β phase stability. As schematically depicted in Figure 1, the deformation of traditional high-strength Ti alloys is dominated by dislocation slipping owing to the high β phase stability, leading to a high yield strength but low uniform elongation and limited strain hardening [13]. As the yielding of the materials under deformation is controlled by the initiation of the dominant deformation mode, the activation of twinning

and stress-induced phase transformation resulted in a decrease in yield strength due to their lower trigger stress. Generally, the relationship between the trigger stress of dislocation slipping (σ_{slip}), deformation twinning ($\sigma_{twinning}$), and stress-induced martensitic transformation (σ_{SIMT}) is $\sigma_{slip} > \sigma_{twinning} > \sigma_{SIMT}$. Thus, the alloys with a solo TWIP effect (TWIP Ti) exhibit a higher yield strength than the alloys with combined TRIP and TWIP effects (TWIP/TRIP Ti) and the solo TRIP effect (TRIP Ti) [7,12,24,34,37–40].

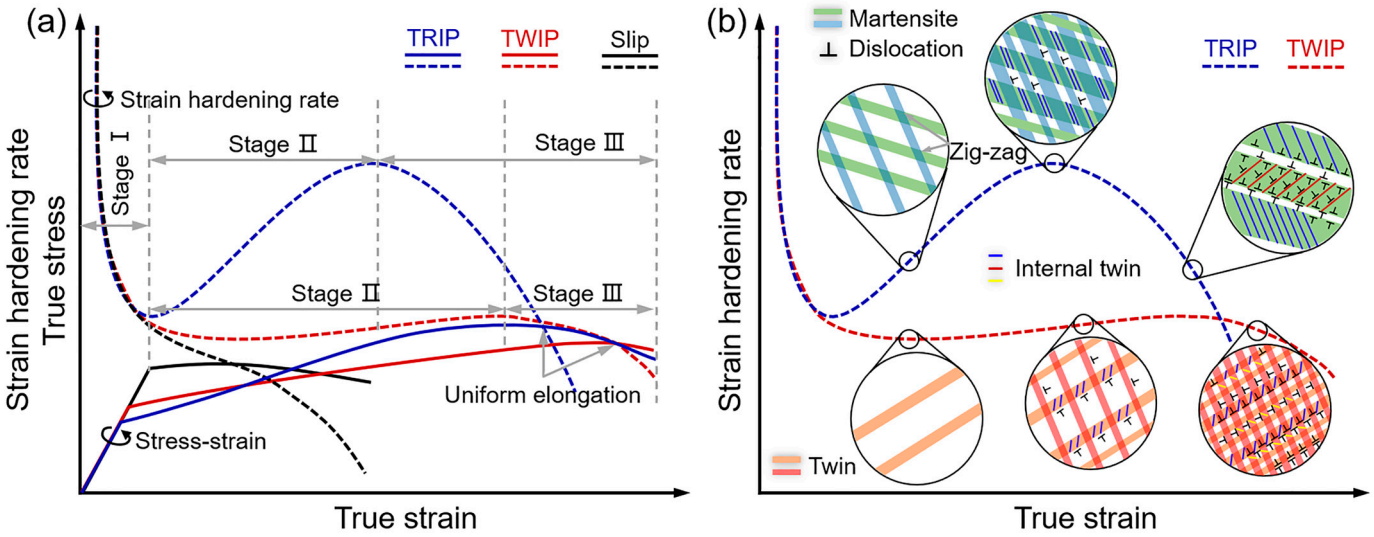

Figure 1. Schematic illustration of the (**a**) strain hardening behaviors and (**b**) deformation mechanisms of the TRIP and TWIP Ti alloys.

The harnessing of dynamic phase transformation and deformation twinning is manifest by generating abundant phase/twinning boundaries to effectively impede the dislocation motion. This leads to remarkable strain hardening via the dynamic Hall–Petch effect, as schematically demonstrated in Figure 1b. TRIP/TWIP Ti alloys possess an exceptional ability to delay strain localization, preventing plastic instability and necking owing to their excellent strain hardening capability. Their strain hardening behavior is directly related to the kinetics of TRIP and TWIP effects, which resembles a three-stage way [6,41,42]. The strain hardening rate increases rapidly to a local maximum value or almost remains unchanged due to the formation of martensite or twinning during stage II, respectively. Subsequently, it exhibits a downward trend until the fracture of the material, attributing to the near supersaturation of the deformation-induced products and initiation of dislocation slipping-dominated deformation.

The TRIP effect, characterized by the rapid formation of the martensitic phase, introduces abundant phase boundaries and quickly refines the prior coarse β grains into smaller martensite-free β blocks. Consequently, dynamic strengthening via the TRIP effect is more effective than the TWIP effect [43], which proceeds slowly and within a wider range of strain (as shown in Figure 1a). The strain hardening capability of TRIP/TWIP alloys primarily depends on the formation rate of deformation products and their interactions with dislocations. The sharp martensitic transformation, which predominately occurs at strains lower than 5% [23,24,44], leads to a rapid strain hardening response and, thus, a higher strain hardening rate. However, the strain hardening rate drops rapidly after reaching near supersaturation and dislocation-controlled yielding of the stress-induced martensite. This results in a quick decline in strain hardening ability against plastic instability and, thus, a lower uniform elongation of the TRIP Ti alloys compared to the TWIP counterparts [45].

In contrast, the formation kinetics of deformation twinning is more sluggish, proceeding continuously and steadily across a wider range of strains. This leads to a relatively lower strain hardening rate but a superior ability to prevent plastic insatiably [7]. In most cases, both the TRIP and TWIP are activated in TRIP/TWIP Ti alloys, with the

stress-induced martensitic transformation occurring before the activation of deformation twinning [12,17,27].

In the early deformation stage of TRIP/TWIP Ti alloys, the stress-induced martensite and deformation twinning, including {332}<113>$_\beta$ twinning and {112}<111>$_\beta$ twinning, exhibit a favorite crystallographic orientation concerning the applied stress axis [46]. They initially nucleate at the β grain boundaries and grow across the whole grain until they encounter other β grain boundaries, as is shown in Figure 1b [19]. With increasing strain/stress, additional martensite/twin variants with different crystal orientations are activated and interact with the initially formed ones. This interaction results in a zig-zag configuration, effectively dividing the prior coarse β grains into fine martensite/twin-free β blocks [8,34]. This process remarkably reduces the average free path available for dislocation slipping and hinders the dislocation motion, leading to effective strengthening as a result of the dynamic Hall-Petch effect.

Unlike deformation twinning, stress-induced martensitic transformation proceeds rapidly at low strain, and internal twins usually formed at locations where the martensite variants intersect (zig-zag configuration), leading to a rapid strain hardening response [8,19,20]. Internal martensite twinning, {332}<113>$_\beta$ twinning and/or {112}<111>$_\beta$ twinning, including secondary twinning and tertiary twinning depending on the modified orientation factor because of the formation of the primary/secondary twinning plane, may also form within the primary martensite/{332}<113>$_\beta$ twins [7,16,47]. With increasing strain/stress, the coarsening/coalescence of the primary martensite with the favorite orientation (highest Schmid factor) occurs by the growth of the primary martensite and the consumption of the non-favorite variants (reorientation) [8,20]. Consequently, the majority of a prior β grain is occupied by the coarsened martensite in TRIP Ti alloys [8]. Finally, dislocation slipping can be initiated within the coarsened martensite.

As for TWIP Ti alloys, there is no significant coarsening of the twin variants, but the continuous formation of twinning variants and internal secondary twinning and tertiary twinning occurs before the dislocation-dominated plastic deformation [14,48]. When the local maximum strain hardening rate is reached in stage II, the initial β matrix is mainly transformed into martensite or twins. Afterward, the strain hardening rate decreases significantly, leading to plastic instability in TRIP/TWIP Ti alloys. Most of the TRIP/TWIP Ti alloys deform through hybrid stress-induced martensitic phase transformation and deformation twinning, with the stress-induced martensitic transformation occurring before deformation twinning [6]. One drawback of these TRIP/TWIP Ti alloys is their relatively low yield strength owing to the low trigger stress of stress-induced martensitic transformation [12,49,50].

The strain hardening capability and uniform elongation of TRIP/TWIP Ti alloys are closely linked to the dynamic phase transformation/twinning kinetics during deformation. To achieve a combination of high yield strength, strong strain hardening capability, and high uniform elongation, it is necessary for the dynamic phase transformation/twinning to proceed relatively slowly and continuously within a wide range of strains while maintaining the transformation/twinning degree of the β matrix almost unchanged. This can be achieved through various methods such as ω phase precipitation [5,18,51], α phase precipitation [17], and pre-straining induced twinning [52,53]. These methods create obstacles that impede the propagation of the stress-induced martensite and deformation twinning, thus slowing down the dynamic phase transformation/twinning kinetics. This provides an opportunity for the microstructure-guided design of high-performance TRIP/TWIP Ti alloys via fine-tuning the dynamic phase transformation and twinning behavior.

2.2. Role of β Phase Stability

The deformation mechanism of single β phase Ti alloys is primarily determined by the lattice stability of the β phase, which is related to their chemical compositions. Figure 2 shows schematically the evolution of the deformation mode with increasing β phase stability, in which the transition from stress-induced martensitic phase transformation (TRIP),

combined stress-induced martensitic phase transformation and deformation twinning (TRIP/TWIP), deformation twinning (TWIP), and dislocation slipping are activated to accommodate the increasing β phase stability [49,54]. As the chemical composition (β phase stability) of the metastable β-Ti alloys is fixed, their deformation mechanisms and, thus, mechanical behaviors are predictable after β-solution treatment and water quenching. This provides the basis for the compositional design and prediction of the deformation modes of metastable β-Ti alloys using the $\overline{Bo}$-$\overline{Md}$ phase stability diagram initially proposed by Morinaga et al. [55] and modified by Abdel-Hady et al. [56]. A series of high-performance TRIP/TWIP Ti alloys, such as Ti-9Mo-6W [57], Ti-8.5Cr-1.5Sn [4], Ti-3Al-5Mo-7V-3Cr [13], Ti-4Mo-3Cr-1Fe [7], and Ti-6Mo-3.5Cr-1Zr [58], have been designed and developed by adjusting the chemical compositions based on considering the role of the β-stabilizing effect, the changing trend of the $\overline{Bo}$ and $\overline{Md}$ values, and the solid-solution strengthening effect of the alloying elements.

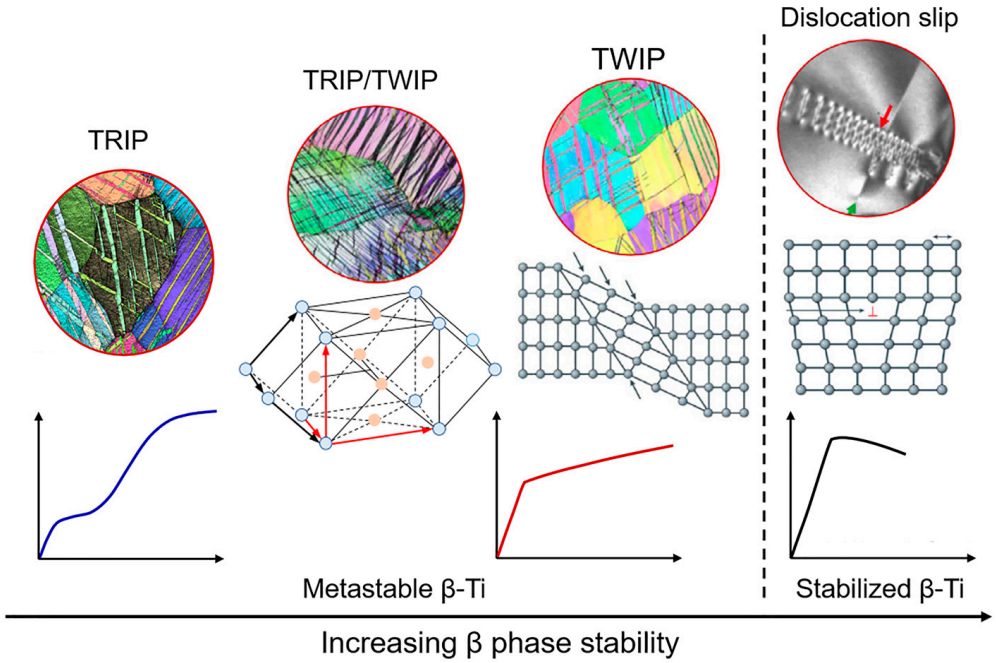

Figure 2. Evolution of the deformation modes with the increasing β phase stability of β-Ti alloys. (Reprinted with permission from Ref. [54]. Copyright 2022, Elsevier).

Additionally, the deformation modes and mechanical properties of the same metastable β-Ti alloy can also be tuned by diffusional precipitation of the α phase and ω phase, which changes the chemical compositions and, thus, the stability of the retained β matrix. This occurs as the β-stabilizers are enriched in the retained β matrix. As such, the deformation mode and mechanical properties of the metastable β-Ti alloy can be tuned, leading to the development of α/ω precipitation strengthened TRIP/TWIP Ti alloys [5,18,59]. This changes the deformation modes and mechanical properties of the TRIP/TWIP Ti alloys, which leads to increased yield strength and ultimate tensile strength but decreased ductility and strain hardening capacity as a result of the transition or suppression of the TRIP and/or TWIP effect.

2.3. Role of α″ Martensite and α′ Martensite

2.3.1. Stress-Induced β-to-α″ Martensitic Transformation

The stress-induced α″ martensite plays an important role in the TRIP/TWIP Ti alloys not only by rendering the alloys with simultaneously enhanced strength and ductility but also by acting as an assisting role in the formation of deformation twinning. It is reasonable that the low β phase stability and low triggering stress of stress-induced martensite phase

transformation favor the formation of α'' martensite at low applied stress that is lower than the trigger stress of deformation twinning. The formation of stress-induced α'' martensite in conjunction with the deformation twinning was usually observed during the early-stage deformation of the TRIP/TWIP Ti alloys [6]. It is worth noting that the fraction of α'' martensite formed at the early deformation stage of TRIP/TWIP Ti alloys is significantly lower than that of the pure TRIP Ti alloys. Nevertheless, it contributes largely to the strain hardening and the overall deformation mechanisms of the TRIP/TWIP Ti alloys.

Recent research using in situ synchrotron X-ray diffraction [60,61], crystallographic orientation analysis based on electron backscattered diffraction (EBSD) [27,62] and transmission electron microscopy (TEM) [44], and high-resolution TEM (HRTEM) [63,64], has revealed that the formation of $\{332\}_\beta$ twining is closely related to the formation and reversion of α'' martensite during stress loading and unloading, respectively. It is documented that a parent $\{130\}\langle 310\rangle_{\alpha''}$ twinning system was firstly formed at the early deformation stage, which transformed to $\{332\}_\beta$ twinning after the reversion of α''-to-β upon stress release [27,60,64].

Note that the $\{332\}_\beta$ twinning system is not energetically favorable in comparison to $\{112\}_\beta$ twinning in bcc metals due to the additional movement of atoms to form $\{332\}_\beta$ twinning [65]. However, it is $\{332\}_\beta$ twinning other than $\{112\}_\beta$ twinning more frequently formed in TRIP/TWIP Ti alloys. The reduction in the β phase stability reduces its shear modulus c', which reflects the lattice instability against shuffling of the $\{0\bar{1}1\}_\beta$ planes along the $\langle 011\rangle_\beta$ direction, i.e., $\{0\bar{1}1\}\langle 011\rangle_\beta$ shuffling that is required for the β-to-α'' martensitic phase transformation [66]. Therefore, stress-induced β-to-α'' martensitic transformation is more likely to occur at low trigger stress in TRIP/TWIP Ti alloys. This lattice instability facilitates the formation of the stress-induced β-to-α'' martensitic transformation with a $\{130\}\langle 310\rangle_{\alpha''}$ twinning, which corresponds to the $\{332\}\langle 11\bar{3}\rangle_\beta$ twinning of the parent β phase according to the lattice correspondence between the α'' and β [65]. Thus, stress-induced α'' martensite in conjunction with $\{332\}\langle 11\bar{3}\rangle_\beta$ twinning was usually observed in TRIP/TWIP Ti alloys.

The relatively low yield strength of TRIP/TWIP Ti alloys can be attributed to the easy activation of stress-induced β-to-α'' martensitic transformation at low applied stress. Stress-induced internal secondary α'' martensitic can also form inside the primary $\{332\}_\beta$ twins or at $\{332\}_\beta$ twin interface [15,32,67,68]. Except for $\{332\}_\beta$ twinning, the stress-induced α'' martensite can also assist the formation of $\{112\}_\beta$ twining through the formation of $\{110\}\langle 110\rangle_{\alpha''}$ twinning and its reversion [69,70]. The complex interplay between the stress-induced α'' martensitic transformation and deformation twinning renders new opportunities for designing new TRIP/TWIP Ti alloys. This can be achieved by tailoring the chemical composition (β phase stability) to simultaneously promote the activation of stress-induced α'' martensite, $\{332\}_\beta$ twinning, and $\{112\}_\beta$ twining during deformation. It is also pertinent to manipulate the stress-induced martensitic phase transformation behavior to make it sluggishly and continuously proceed over a wide range of strain, aiming to obtain a synergetic combination of high yield strength, high ductility, and high strain hardenability. Some feasible ways are demonstrated as ω precipitation [5,18,51], α precipitation [15,17], grain refinement [17,18,71], solid-solution strengthening [13,26,49], and/or heterogeneous microstructure design [72,73], which increased the trigger stress required to initiate stress-induced martensitic phase transformation and reduced the transformation kinetics by acting as barriers for the initiation and propagation of the stress-induced phase transformation and deformation twinning.

2.3.2. Stress-Induced β-to-α' Martensitic Transformation

Except for orthorhombic α'' martensite, hexagonal close-packed (hcp) α' martensite can also be induced during the deformation of metastable β-Ti alloys [20,74,75]. This introduces a new class of TRIP/TWIP Ti alloys based on stress-induced β-to-α' martensitic transformation [8]. Unlike the α'' martensite that can deform easily through processes like reorientation and dislocation slipping, the limited slip systems of the α' martensite make

it more effective at imparting high strain hardening over those reliant on stress-induced β-to-α″ martensite. These TRIP/TWIP Ti alloys with stress-induced β-to-α′ martensitic transformation have been reported to exhibit a synergetic combination of high strength, high ductility, and high strain hardening capability, as demonstrated in Ti-15Nb-5Zr-4Sn-1Fe [8], Ti-4Al-4Fe-0.25Si-0.1O [20], Ti-4Al-2Fe-1Mn [76] TRIP Ti alloys, and Ti-rich high entropy alloys [77,78]. The high strain hardening ability and high strength of stress-induced β-to-α′ martensitic transformation originates from the hierarchically formed α′ martensite with multiple secondary and tertiary variants, as well as internal twins. These features, along with their complex interplay with dislocation slipping, contribute to the exceptional mechanical properties of this class of Ti alloys [8].

As β-to-α″ transformation lies as an intermediary on the pathway of β-to-α′ martensitic transformation [79,80], the trigger stress required to activate stress-induced β-to-α′ martensitic transformation is reasonably higher than that of the stress-induced β-to-α″ martensite. TRIP/TWIP Ti alloys based on stress-induced β-to-α′ martensitic transformation can, thus, harness higher yield strength than those reliant on stress-induced β-to-α″ martensite, offering an alternative way to overcome the low yield strength of the TRIP/TWIP Ti alloys. Owing to the lattice correspondence between the α″ and α′, the dynamic phase transformation from α″-to-α′ can occur during deformation, based on which a new type of TRIP Ti alloys can be developed [23,81–84]. However, under what chemical composition (β phase stability) can β-to-α′ martensitic transformation occur is not well understood. This knowledge gap creates difficulty in the compositional designing and development of new TRIP Ti alloys that rely on stress-induced β-to-α′ martensitic transformation.

One factor to consider is the chemical composition, specifically the β phase stability, which can significantly influence the occurrence of stress-induced β-to-α′ martensitic transformation. It is worth noting that Ti alloys do not exhibit a strong propensity for stress-induced β-to-α′ martensitic transformation, as stress-induced β-to-α″ martensitic transformation dominates. This makes the mechanism of dynamic transformation from β-to-α′ during deformation not fully understood yet. Fu et al. [8] indicate that stress-induced β-to-α′ martensitic phase transformation is accompanied by the disappearance of the athermal ω phase, while Lee et al. [19,20] suggest a close correlation between the O′ phase with stress-induced β-to-α′ martensitic phase transformation and its twinning. Further research is necessary to elucidate the intricate deformation mechanisms involved in this transformation.

2.4. Role of ω Phase

2.4.1. Effect of ω Phase on Stress-Induced Martensitic Transformation and Deformation Twinning

The presence of the ω phase does not necessarily lead to brittleness in Ti alloys, especially in TRIP/TWIP Ti alloys. Owing to the low phase stability of the TRIP/TWIP Ti alloys, the β phase usually transforms to the nanoscale athermal ω (ω_{ath}) phase after solution treatment and fast cooling. The chemical composition of this ω_{ath} phase is identical to that of the parent β phase (supersaturated) and is highly coherent with the β matrix [85–87]. Different from the isothermal ω (ω_{iso}) phase that forms under isothermal aging, the ω_{ath} phase, when present, tends not to suppress stress-induced martensitic phase transformation and deformation twinning. Instead, it may potentially act as an assistant role in promoting stress-induced martensitic phase transformation and deformation twinning in some ways. However, ω_{iso} formed via artificial aging at elevated temperature partially or fully suppressed the stress-induced β-to-α″ transformation and deformation twinning, thus changing the deformation mechanism from TRIP-dominated to TWIP-dominated or even dislocation slipping, resulting in a significant reduction in ductility or even brittleness [18,88–91].

It has been frequently observed that the ω_{ath} phase fully vanished following the formation of stress-induced α′ martensite or α″ martensite [5,8,16,22], while the disappearance of one variant of the ω_{ath} phase particles was usually observed after the formation of the

$\{332\}_\beta$ and $\{112\}_\beta$ deformation twinning [7,14,92]. The presence of the dense ω_{ath} phase disrupts the continuance of the β matrix, acting as a strong obstacle to stress-induced phase transformation and deformation twinning of the β matrix. It is expected that during deformation, the ω_{ath} phase may revert back to the parent β phase (ω-to-β reversal mechanism). Subsequently, the stress-induced β-to-α''/α' martensitic transformation takes place within the ω-free β matrix [5,93]. This phenomenon of the disappearance of the one variant of the ω_{ath} phase, accompanied by the emergence of $\{332\}_\beta$ and $\{112\}_\beta$ mechanical twinning, may be highly related to dislocation slipping. Based on both theoretical and experimental results, it is proposed that partial dislocations slipping on the successive $\{10\bar{1}0\}_\omega$ ω planes lead to the formation of $\{112\}_\beta$ twinning [94,95]. The ω-to-β reversal mechanism controlled microstructure evolution sequence during deformation can be summarized as follows: $\beta + \omega_{ath} \rightarrow \beta \rightarrow$ martensite/$\{112\}_\beta$ twinning. If this proposed mechanism is true, the reversibility of the ω phase could undoubtedly have a significant impact on the dynamic phase transformation and twinning behaviors exhibited in TRIP/TWIP Ti alloys. Further research is warranted to fully elucidate the underlying mechanisms and their implications for mechanical properties.

The reversibility or the effect of the ω phase on the dynamic phase transformation and deformation twinning is closely related to the shear modulus (chemical composition) of the ω phase [85]. Accordingly, the kinetics of phase transformation and twinning during deformation can be adjusted by fine-tuning the precipitation of the ω_{iso} phase through isothermal aging at elevated temperatures. This process is accompanied by the rejection of the solute atoms from the supersaturated ω_{ath} phase into the surrounded β matrix, a phenomenon known as elemental partitioning. The rejection of the β-stabilizers increases the shear modulus [85,89] and internal elastic strain energy of the ω_{iso} phase, making them hard and even undeformable [96,97], thereby suppressing the stress-induced martensitic phase transformation and deformation twinning. This may also be due to the decreased ω-to-β reversibility as a result of solute atom partitioning [51]. Consequently, it becomes possible to induce a sluggish process of stress-induced martensitic transformation and deformation twinning by finely tuning the precipitation of the ω phase. This, in return, would result in a decreased strain hardening rate, thus delaying the occurrence of the stress localization, ultimately increasing the uniform elongation [51].

2.4.2. Tuning Mechanical Properties by Engineering ω Precipitation

As the apparent yield strength of TRIP/TWIP Ti alloys is primarily determined by the trigger stress required to activate stress-induced martensitic phase transformation and/or deformation twinning, the presence of dense ω_{ath} particles will not significantly enhance the yield strength [98]. Conversely, the precipitation of ω_{iso} particles substantially enhances the yield strength as a result of precipitation strengthening, increased trigger stress to activate the specific deformation mode, and altered deformation modes due to the change in the phase stability of the β matrix. Therefore, a significant enhancement in yield strength, while synergistically maintaining the ductility or even enhancing uniform elongation, can be achieved by fine-tuning the precipitation, growth, and solute atom partitioning of the isothermal ω phase. The successful application of ω strengthening in TRIP/TWIP Ti alloys has been demonstrated by short-time aging (1 min) at low temperature (200 °C) in Ti-12Mo alloy [18,99], isothermal aging at 200 °C in Ti-5Al-3Mo-3V-2Cr-2Zr-1Nb-1Fe [25], and natural aging at room temperature in Ti-10V-2Fe-3Al [5] and Ti-15Nb-5Zr-4Sn-1Fe [51]. It is important to note that the successful application of ω strengthening, whether by artificial aging or natural aging, highly relies on the precise control of the aging temperature and duration. These factors dictate the content of precipitation and solute atom partitioning of the ω phase. Additionally, low-temperature short-term aging is not suitable for large-size or thick plate components owing to the limited thermal conductivity of Ti alloys and potential differences in thermal exposure across a part [51].

Simultaneous enhancements in yield strength and uniform elongation have been documented in a TRIP Ti-15Nb-5Zr-4Sn-1Fe alloy subjected to natural aging. The diffusional

growth of the ω_{ath} particles during natural aging serves to hinder the deformation-induced ω_{ath}-to-β reversion and stress-induced β-to-α′ martensitic transformation while slightly promoting the stress-induced β-to-α″ transformation. As a result, the stress-induced β-to-α′ martensitic transformation can take place continuously over a wider range of strains than the alloy without natural aging [51]. This approach is also likely to be applicable to other TRIP/TWIP Ti and TWIP Ti alloys. Natural aging presents a new method for regulating stress-induced martensitic transformation and deformation twinning, thereby enhancing the mechanical properties of TRIP/TWIP Ti alloys by controlling the development of the ω_{ath} phase.

2.4.3. Stress-Induced β-to-ω Transformation

Deformation in metastable β-Ti alloys can also be accommodated by stress-induced β-to-ω phase transformation. A subclass of TRIP Ti alloys has been developed based on stress-induced β-to-ω phase transformation. This class of TRIP Ti alloys demonstrates an excellent combination of mechanical properties, like Ti-9Cr-0.2O [28,100] and Ti-6Mo-3.5Cr-1Zr [29,58]. By introducing stress-induced plate-shaped ω phase transformation to replace the stress-induced β-to-α″ transformation, it becomes possible to overcome the low yield strength of the traditional TRIP/TWIP Ti alloys. For instance, a high yield strength of 698 MPa and high uniform elongation of 32% have been achieved in the Ti-6Mo-3.5Cr-1Zr alloy. These superior properties were harnessed by the coupled effects of TRIP (stress-induced β-to-ω phase transformation), TWIP ($\{332\}_\beta$ twinning), and their interaction with dislocations [58].

3. Compositional Design of TRIP/TWIP Ti Alloys

Based on the numerical statistics of the chemical composition (β phase stability)-dependent activation of stress-induced phase transformation (TRIP) and deformation twinning (TWIP), the deformation mechanism of TRIP/TWIP Ti alloys is intricately linked to their chemical compositions. This relationship enables the compositional design of TRIP/TWIP Ti alloys via a knowledge-based semi-empirical modulation of the β phase stability through alloying, guided by *d*-electron theory, electron-to-atom ratio (e/a) method, and molybdenum equivalent ($[Mo_{eq}]$).

3.1. d-Electron Theory

The last decade has witnessed the discovery of TRIP/TWIP Ti alloys with the aid of the $\overline{Bo}$-$\overline{Md}$ map based on the *d*-electron theory proposed by Morinaga et al. [101]. After calculating the electronic parameters of bond order (Bo) and metal *d*-orbital energy level (Md) of each alloying element using the DV-Xα cluster molecular orbital method, the mean $\overline{Bo}$ and $\overline{Md}$ parameters of the alloy can be approximated via compositional averaging:

$$\overline{Md} = \sum_{i=1}^{n} x_i (Md)_i \quad (1)$$

$$\overline{Bo} = \sum_{i=1}^{n} x_i (Bo)_i \quad (2)$$

where x_i is the atomic fraction of element i in the alloy.

A $\overline{Bo}$-$\overline{Md}$ map has been constructed, and the map is divided into different regions based on the correlation between the mean electrical parameters and deformation modes of Ti alloys, as is shown in Figure 3. A metastable β-Ti alloy can be obtained when locating it at the left side of the $M_s = RT$ line, where M_s represents the martensite start transformation temperature, and RT corresponds to room temperature. Two distinguished zones are divided by the $M_d = RT$ boundary, where the combined TRIP and TWIP (TRIP/TWIP Ti) are reported to occur (Figure 3a). High-performance TRIP/TWIP Ti alloys have been successfully designed by adjusting the chemical composition to tailor the $\overline{Bo}$ and $\overline{Md}$ parameters [4,7,12,13,34,37,41,48,57,59,68,102–107]. As illustrated in Figure 3a, the deformation modes of most designed TRIP/TWIP alloys align with predictions from the $\overline{Bo}$-$\overline{Md}$ map, showing its effectiveness in TRIP/TWIP Ti alloy design. Nevertheless, deviation

in activated deformation mode from the predicted one by the $\overline{Bo}$-$\overline{Md}$ map has also been reported due to the limitation in considering the interaction between alloying elements when calculating the mean electric parameters. For example, both the Ti-4Mo-4Co (at. %) and Ti-6Mo-4Zr (at. %) are located in the twinning region, but they exhibit significant differences in mechanical properties and deformation mechanisms. Ti-6Mo-4Zr showed both TRIP and TWIP behaviors, while Ti-4Mo-4Co did not [108]. This indicates that accurately predicting the deformation modes of some metastable β-Ti alloys using the current $\overline{Bo}$-$\overline{Md}$ map, especially for complex multicomponent systems, can be challenging due to the complex interaction among alloying elements that change the electric state and phase stability of the β phase.

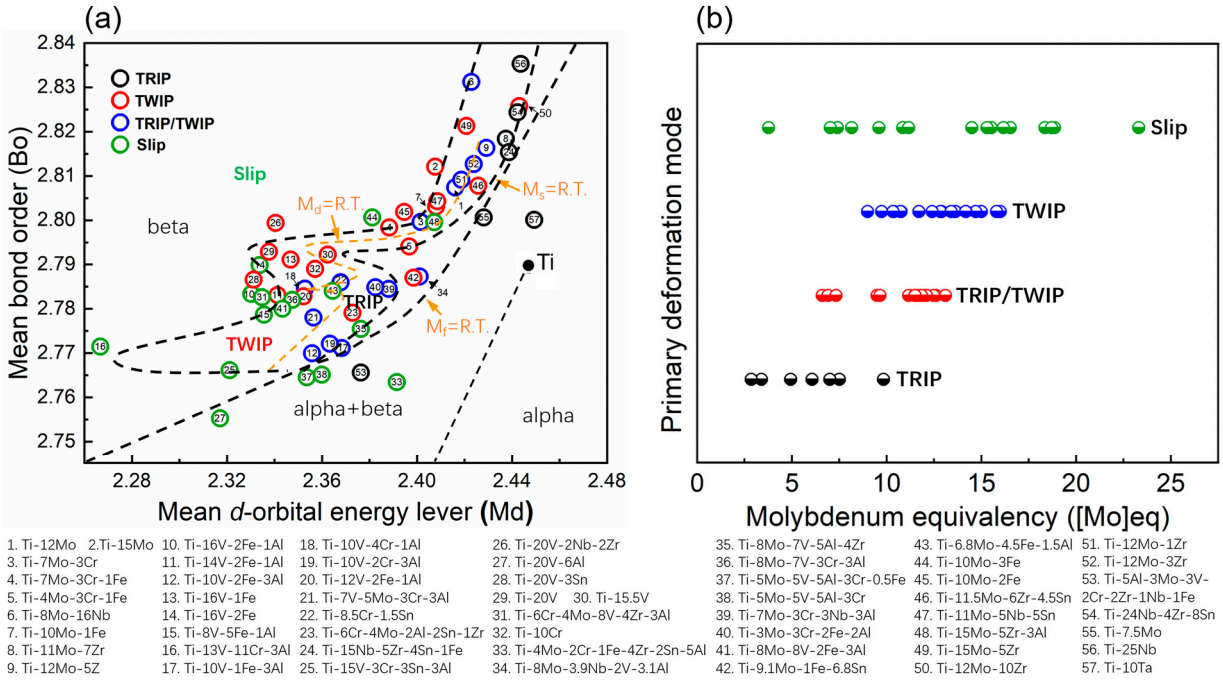

Figure 3. (**a**) $\overline{Bo}$-$\overline{Md}$ map and (**b**) $[Mo]_{eq}$ showing the relationship between the deformation mechanisms and $\overline{Bo}$, $\overline{Md}$, and $[Mo]_{eq}$ of metastable β-Ti alloys based on experimental results.

For the improved application of *d*-electron theory toward the highly efficient compositional design of TRIP/TWIP Ti alloys, it is advisable to refine the boundary of the current $\overline{Bo}$-$\overline{Md}$ map by synthesizing available alloy datasets, as presented by Abdel-Hady et al. [16] and Bignon et al. [109]. It is plausible to combine the *d*-electron theory with additional methods, like the molybdenum equivalent ($[Mo]_{eq}$) [110], electron-to-atom ratio (e/a) method [108], and machine learning, to more accurately indicate the relationship between the activatable deformation modes and chemical compositions of metastable β-Ti alloys.

3.2. Molybdenum Equivalent ($[Mo]_{eq}$)

The molybdenum equivalent ($[Mo]_{eq}$) is proportional to the β phase stability and, thus, can offer a rough estimate of the deformation modes in metastable β-Ti alloys. Li et al. [111] demonstrated that when the $[Mo]_{eq}$ falls within the range of 9 to 16, metastable β-Ti alloys are most likely to undergo stress-induced β-to-α″ martensite transformation. A high $[Mo]_{eq}$ supports dislocation slipping while suppressing TRIP and TWIP mechanisms. Figure 3b summarizes the deformation modes of β-Ti alloys based on $[Mo]_{eq}$ values. It becomes evident that deformation modes transition sequentially from TRIP to TRIP/TWIP, then to TWIP, and finally to the dislocation slipping with increasing $[Mo]_{eq}$ [112]. TRIP predominates when $[Mo]_{eq}$ is below 10, while TRIP/TWIP and TWIP are more likely to be achieved if the $[Mo]_{eq}$ is between 6 to 13 and 9 to 16, respectively. This underscores the practical utility of $[Mo]_{eq}$ in the design of TRIP/TWIP Ti alloys. However, it should

be pointed out that Ti alloys with $[Mo]_{eq}$ between 7 and 16 can exhibit a dislocation slip-dominated deformation mechanism. This discrepancy arises from the complex elemental interaction in influencing the β phase stability and deformation mechanisms of Ti alloys.

The classic formula for calculating $[Mo]_{eq}$ is developed by Bania [113] and is expressed as follows:

$$[Mo]_{eq}^{Bania} = 1Mo + 0.67V + 0.44W + 0.22Ta + 1.6Cr + 0.28Nb + 2.9Fe + 1.54Mn + 1.25Ni - [Al]_{eq} \quad (3)$$

where $[Al]_{eq}$ represents the aluminum equivalent. This empirical formula for $[Mo]_{eq}$ only considers the β-stabilizing effect of individual β-stabilizing elements on Ti. However, metastable β-Ti alloys often stabilize the β phase by incorporating multiple elements, such as Mo, Cr, Zr, and Sn. Indeed, the addition of multiple elements in combination, along with their complex interactions, can alter the β-stabilizing effect of each element. Wang et al. [114] took into account the combined presence of multiple elements and the β-stabilizing effects of Zr and Sn, and they modified the $[Mo]_{eq}$ coefficients as follows:

$$[Mo]_{eq}^{Wang} = 1.0Mo + 1.25V + 0.59W + 0.28Nb + 0.22Ta + 1.93Fe + 1.84Cr + 1.50Cu + 2.46Ni + 2.67Co + 2.26Mn + 0.30Sn + 0.47Zr + 3.01Si - 1.47Al \quad (4)$$

The modified $[Mo]_{eq}$ formula takes into consideration the β-stabilizing effects of elements like Nb, Zr, and Sn when added together, making it more representative of the actual β stability compared to traditional $[Mo]_{eq}$ formulas.

3.3. $\overline{e/a} - \overline{\Delta r}$ Diagram

A semi-empirical approach was proposed by Wang et al. [108] for predicting the twinning propensity of metastable β-Ti alloys. This method takes into account both the mean electron-to-atom ($\overline{e/a}$) and the compositional average of the difference in atomic radii between the Ti element and other alloying elements ($\overline{\Delta r}$). The deformation modes of metastable β-Ti alloys are not solely determined by the *d*-electron theory but are also highly related to the $\overline{e/a}$ and $\overline{\Delta r}$ of the alloys. $\overline{e/a}$ and $\overline{\Delta r}$ are calculated as follows:

$$\overline{e/a} = \sum_{i=1}^{n} N_i c_i \quad (5)$$

$$\overline{\Delta r} = \sum_{i=1}^{n} c_i (r_i - r_{Ti}) \quad (6)$$

in which N_i and r_i are the numbers of valence electrons and atomic radius of the element i, r_{Ti} is the atomic radius of Ti, and c_i is the atomic percentage of element i.

Both the stress-induced martensitic phase transformation and mechanical twinning require a shear component of the β lattice. Thus, the likelihood of stress-induced martensitic transformation and deformation twinning is closely related to the shear modulus c' of the β phase, which reflects the lattice shear stiffness and stability of the β phase. Experimental and first-principle calculation results indicate that c' and β phase stability decrease with decreasing $\overline{e/a}$ [115]. After correlating the deformation modes with $\overline{e/a}$ and $\overline{\Delta r}$ of more than 50 Ti alloys following solution treatment, a $\overline{e/a}$-$\overline{\Delta r}$ diagram was proposed, in which the slip and twinning/slip zones are separated by dashed lines, as shown in Figure 4. It is suggested that a $\overline{\Delta r}$ higher than −2.5 and a $\overline{e/a}$ lower than 4.2 favors the activation of deformation twinning and stress-induced martensitic transformation by reducing the resistance to lattice shear [108]. This semi-empirical diagram successfully predicted the deformation modes of the Ti-4Mo-4Co (at. %) and Ti-6Mo-4Zr (at. %) alloys. The discovery of Ti-25Nb-8Zr-2Zr [116] and Ti-25Nb-1Sn-2Cr [117] TWIP Ti alloys using this method validate its effectiveness in TWIP Ti alloy design. Nevertheless, a certain limitation should exist when predicting the deformation mode of new alloys using this $\overline{e/a}$-$\overline{\Delta r}$ diagram, especially for multicomponent alloy systems, since its slip/twinning boundary was drawn based on existing results.

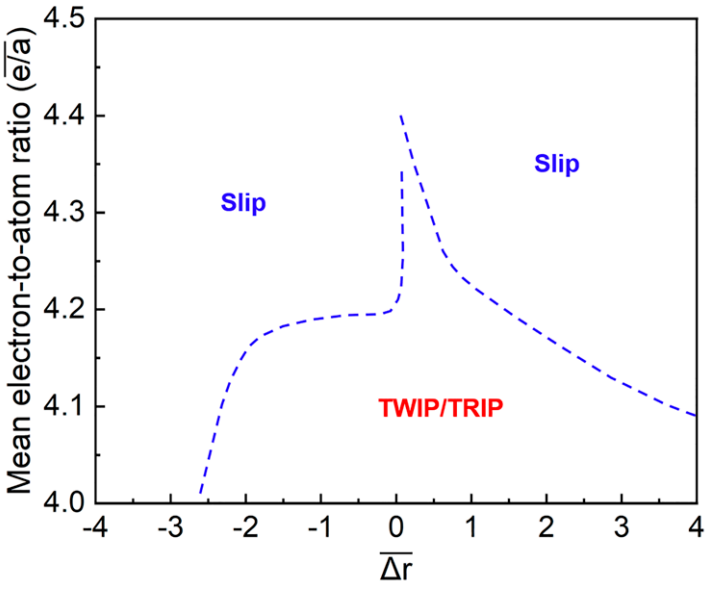

Figure 4. The e/a ratio-$\overline{\Delta r}$ diagram for β-type Ti alloys. (Reprinted with permission from Ref. [108]. Copyright 2019, Elsevier).

It is important to acknowledge that the calculation of $\overline{Bo}$, $\overline{Md}$, $\overline{e/a}$, and $[Mo]_{eq}$ are based on the influence of the individual alloying element (M) on the β phase stability of Ti-M binary alloys, ignoring the interaction among multi-alloying elements [114]. The deviation observed between experimental deformation modes, and those predicted using *d*-electron theory, $\overline{e/a}$, and $[Mo]_{eq}$ are attributed to the complex interaction between multi-alloying elements, which collectively change and enhance the β phase stability. These interactions are not considered in the semi-empirical calculation of electronic parameters and $[Mo]_{eq}$. When neutral elements like Zr and Sn, as well as α-stabilizing element O, are added in combination with other β-stabilizing elements, they all contribute to the β-stabilizing effect [110,118–120]. However, this effect is not reflected in electronic parameters and $[Mo]_{eq}$ calculations. Moreover, the developed $\overline{Bo}$-$\overline{Md}$ map, $[Mo]_{eq}$, and $\overline{e/a}$-$\overline{\Delta r}$ maps are valid primarily for β-solution treated Ti alloys, and they do not consider the effect of processing history and microstructure features, like secondary phase (e.g., ω phase) and grain size, on the deformation of the TRIP/TWIP Ti alloys. These methods also cannot predict the mechanical properties, such as strength. Elaborate modification of the boundaries that divide the different deformation mode zones in the current semi-empirical maps and comprehensive utilization of various methods are helpful for the design of new TRIP/TWIP Ti alloys.

3.4. Machine Learning

The conventional trial-and-error approach and semi-empirical methods require extensive experimental verification, which can be both time-consuming and resource-intensive. Recently, the fields of big data, machine learning, and artificial intelligence have started to exhibit significant advantages in the screening of alloy composition and the optimization of processing technology. A data-driven system can facilitate the integrated design of high-performance Ti alloy to address the challenge of high computational complexity and the difficulty of designing multi-element alloys faced in semi-empirical methods and first-principles calculations. This system leverages the power of machine learning to establish implicit relationships within the "composition-process-structure-performance" of materials in unknown space, offering a commonly used strategy for artificial intelligence (AI)-assisted material research and development. The compositional design strategy utilizing machine learning comprises four basic modules: (1) constructing a database; (2) data mining and screening; (3) modeling and machine learning; (4) discovery and design [121].

For instance, an artificial neural network was employed to develop an 883 °C-heat-treated Ti-4Al-2Fe-1.4Mn TRIP alloy with an ultimate tensile strength of 1284 MPa and a fracture elongation of 34%. This development was based on 30 experimental tensile datasets from Ti-4Al-2Fe-xMn (x = 0–4 wt%) alloys heat-treated in the temperature range of 830 °C to 920 °C [122]. Another significant achievement by Wang et al. [123] involved integrating a first principle calculation and cluster model into a machine learning framework to establish a quantitative relationship between "composition-process-performance". This approach allowed for the direct and efficient prediction of mechanical properties based on heat treatment parameters. The integration of machine learning with experimental material technology effectively improves the efficiency and intelligence level in the design of TRIP/TWIP Ti alloys.

4. Development of TRIP/TWIP Ti Alloys

Since the first publication of Ti-12Mo TRIP/TWIP Ti alloy by Marteleur et al. in 2012 [12], which was designed using *d*-electron theory, there has been growing interest in these alloys over the past decade due to their remarkable combination of high strength, high ductility, and high strain hardening rate. Inspired by the compositional design method and complex combination of deformation mechanisms observed in Ti-12Mo alloy, including stress-induced β-to-α′ martensitic transformation, stress-induced β-to-α″ martensitic transformation, and $\{332\}_{\beta}$ deformation twinning [12,26,67], a variety of new TRIP/TWIP Ti alloys with promising mechanical properties were designed using *d*-electron theory. Examples of these alloys include Ti-9Mo-6W [57], Ti-8Cr-1.5Sn [4], and Ti-12Mo-5Zr [106]. These alloys have demonstrated simultaneously enhanced strength and ductility as a result of stress-induced martensitic phase transformation (TRIP) and deformation twinning (TWIP).

For instance, the TRIP/TWIP Ti-8.5Cr-1.5Sn exhibited 3–4 times greater ductility than Ti-6Al-4V and a 50% higher yield strength than Fe-22Mn-0.6C TWIP steel [4]. Nevertheless, the yield strength of Ti-8.5Cr-1.5Sn is about 520 MPa, and it is about 480 MPa for Ti-12Mo [4]. The design and development of new TRIP/TWIP Ti alloys have recently been a significant research focus in the Ti community. In addition to ternary alloys, Ti-Mo [17,91,124], Ti-Nb [8,125], Ti-V [13,96,105], and Ti-Cr [17,68] based multi-component alloys have been developed, such as Ti-6Cr-4Mo-2Al-2Sn-1Zr (Ti-64221) [14], Ti-3Al-5Mo-7V-3Cr (Ti-3573) [13], and Ti-3Mo-3Cr-2Fe-2Al [17]. More detailed information about the chemical compositions, deformation mechanisms, and mechanical properties of these developed TRIP/TWIP Ti alloys can be found in References [41,43,50].

Table 1 summarizes some recent findings on TRIP/TWIP Ti alloys and their mechanical properties. Researchers are committed to discovering new TRIP/TWIP Ti alloys through compositional design and studying their deformation mechanisms and mechanical properties. Despite the excellent combination of high strength, high ductility, and high strain hardening capability, one of the limitations of the TRIP/TWIP Ti alloys is the inherently soft nature of the parent β phase, which leads to low yield strength (Table 1) owing to the low trigger stress required to initiate stress-induced martensitic transformation and deformation twinning. TRIP/TWIP Ti alloys typically tend to exhibit a yield strength below 600 MPa, for example, Ti-12Mo (~480 MPa) [12], Ti-10V-4Cr-1Al (~420 MPa) [105], and Ti-8.5Cr-1.5Sn (520 MPa) [4], as stress-induced β-to-α″ martensitic transformation is activated at low applied stress. Therefore, the primary challenge lies in enhancing the yield strength of TRIP/TWIP Ti alloys while preserving large ductility and high strain hardenability. Several strategies are proposed to address this challenge and improve the yield strength of TRIP/TWIP Ti alloys. These strategies include solid solution strengthening [7,13,14], the precipitation of secondary phases [15,18,88,99], oxygen interstitial strengthening [26,126–129], and grain refinement [18,130].

Table 1. Summary of the main findings achieved in TRIP/TWIP Ti alloys in recent years with their mechanical properties, including yield strength (YS, MPa), engineering ultimate tensile strength (UTS, MPa), and uniform elongation (uEL).

Alloy (wt.%)	Year	Researchers	Research Findings	YS	UTS	uEL	Ref.
Ti-12Mo (TRIP/TWIP)	2012	M. Marteleur, et al.	Developing a new family of TRIP/TWIP Ti alloys based on *d*-electron alloy design	485	661	0.35	[12]
Ti-12Mo (TRIP/TWIP)	2013	F. Sun, et al.	Unveiling the deformation mechanisms at the early deformation stage in TRIP/TWIP Ti alloy	-	-	0.4	[6]
Ti-15Mo (TWIP)	2013	X. Min, et al.	Quantitative evaluation of $\{332\}_\beta$ twinning at various tensile strains	504	765	0.24	[38]
Ti-10Mo-0.2O (TRIP/TWIP)	2014	X. Min, et al.	Strengthening TRIP/TWIP Ti alloy by oxygen interstitials	800	852	-	[131]
Ti-15Mo (TWIP)	2015	X. Min, et al.	Strengthening TWIP Ti alloy by pre-strain-induced twins and ω_{iso}	760	-	0.15	[132]
Ti-9Mo-6W (TRIP/TWIP)	2015	F. Sun, et al.	Outstanding work hardening and uniform elongation by stress-induced β-to-α″ and β-to-ω transformation and $\{332\}_\beta$ twinning	528	791	0.33	[57]
Ti-9Cr-0.2O (TRIP)	2015	H. Liu, et al.	TRIP by stress-induced β-to-ω transformation	850	1025	0.2	[133]
Ti-27Nb (at.%) (TRIP/TWIP)	2016	P. Castany, et al.	Origin of $\{332\}_\beta$ as a result of reversion of a parent $\{130\}<310>_{\alpha''}$ twinning	-	-	-	[60]
Ti-12Mo (TRIP/TWIP)	2017	F. Sun, et al.	Strengthening TRIP/TWIP Ti alloy through low-temperature aging	730	793	0.38	[99]
Ti-6Cr-4Mo-2Al-2Sn-1Zr (TWIP)	2018	L. Ren, et al.	Ultrahigh product of strength and elongation (42.6 GPa%) by $\{332\}_\beta$ and $\{112\}_\beta$ twinning and reverse ω transformation	670	820	0.31	[14]
Ti-12Mo-5Zr (TRIP/TWIP)	2018	J. Zhang, et al.	Improving yield strength by increasing critical resolved shear stress (CRSS) of stress-induced β-to-α″ transformation	656	733	0.31	[106]
Ti-3Al-5Mo-7V-3Cr (TRIP/TWIP)	2018	S. Sadeghpour et al.	Increasing yield strength by solid-solution strengthening	750	1100	0.19	[13]
Ti-6Mo-4Zr (at.%)	2018	C. Wang, et.al	Introducing a semi-empirical approach based on the average electron-to-atom ratio ($\overline{e/a}$) and atomic radius difference ($\overline{\Delta r}$) to predict the deformation behaviors of metastable β-Ti alloys	475	-	-	[108]
Ti-10V-2Fe-3Al (TRIP/TWIP)	2019	Y. Danard, et al.	Developing design strategy to reach (α + β) dual-phase TRIP/TWIP Ti alloy	670	-	0.30	[15]

Table 1. *Cont.*

Alloy (wt.%)	Year	Researchers	Research Findings	YS	UTS	uEL	Ref.
Ti-18Mo-13Zr (TWIP)	2019	J. Zhang et al.	Multimodal twinning by microscale $\{332\}_\beta$, nanoscale $\{112\}_\beta$, and novel $\{5811\}<135>_\beta$	800	-	0.18	[40]
Ti-4Al-4Fe-0.25Si-0.1O (TRIP)	2019	S. Lee, et al.	Stress-induced β-to-α′ transformation mediated by the O′ phase resulted in an excellent combination of strength and ductility	600	1352	0.3	[19,20]
Ti-11Mo-5Sn-5Nb (TWIP)	2019	G. Zhao, et al.	Building a multiscale dislocation-based model to describe microstructural evolution and strain-hardening of $\{332\}_\beta$ TWIP Ti alloy	490	788	0.24	[41]
Ti-16Nb-8Mo (TRIP/TWIP)	2020	D.M. Gordin, et al.	Designing strain transformable Ti alloy for biomedical applications	420	650	-	[107]
Ti-4Mo-3Cr-1Fe (TWIP)	2020	L. Ren, et al.	Ultrahigh yield strength and ductility harnessed by a stress-induced nano-scale hierarchical twin structure and ω_{ath}-to-β reversion	870	1092	0.27	[7]
Ti-15Nb-5Zr-4Sn-1Fe (TRIP)	2020	Y. Fu, et al.	Designing TRIP Ti alloy with stress-induced β-to-α′ transformation	546	939	0.17	[8]
Ti-10V-2Fe-3Al (TRIP)	2021	B. Ellyson, et al.	β + ω TRIP Ti	-	-	-	[5]
Ti-12Mo (TRIP/TWIP)	2021	B. Qian, et al.	Determining transformation pathways in TRIP/TWIP Ti alloy	-	-	-	[134]
Ti-6Mo-3.5Cr-1Zr (TRIP)	2022	K. Chen, et al.	Designing TRIP Ti alloy with stress-induced β-to-ω transformation	698	1242	0.32	[58]
Ti-12Mo (TRIP/TWIP)	2022	B. Qian, et al.	Strengthening TRIP/TWIP Ti alloy by grain refinement and ω_{iso}	865	-	0.35	[18]
Ti-15Nb-5Zr-4Sn-1Fe (TRIP)	2023	Y. Fu, et al.	Natural aging in TRIP Ti alloy led to simultaneously enhanced yield strength and uniform elongation	683	987	0.17	[51]
Ti-12Mo-0.3O (TRIP/TWIP)	2023	Y. Chong, et al.	Strengthening TRIP/TWIP Ti alloy by grain refinement and oxygen interstitials	826	1064	0.24	[135]

4.1. Solid Solution Strengthening

Solid-solution strengthening by adding substitutional and interstitial elements is a feasible way to improve the yield strength of TRIP/TWIP Ti alloys. The advantages of solid solution strengthening are twofold. The increased yield was obtained in Ti-12Mo-5Zr (656 MPa) [106] and Ti-12Mo-0.18O (623 MPa) [26], compared to baseline Ti-12Mo (480 MPa) due to the solid-solution strengthening effect of Zr and O, respectively. A multi-element Ti-3Al-5Mo-7V-3Cr TRIP/TWIP alloy with an enhanced yield strength of up to 750 MPa was designed based on considering the solid-solution strengthening effect of alloying elements [13]. Furthermore, a TWIP Ti-4Mo-3Cr-1Fe alloy, boasting a high yield strength of 870 MPa, which is the highest among the currently developed TRIP/TWIP Ti alloys [72], was designed by Ren et al. by combined addition of strong solid solution strengthening elements Mo + Cr + Fe [7].

The enhanced yield strength by solid-solution strengthening is also related to the reduced probability or even fully suppressed stress-induced martensitic transformation as a result of improved β phase stability [49]. Therefore, the addition of strengthening elements should be carefully tailored utilizing *d*-electron theory and $[Mo]_{eq}$ to ensure the occurrence of TRIP and/or TWIP effects. A small amount of oxygen interstitial doping can effectively enhance the yield strength by suppressing stress-induced martensitic transformation and deformation twinning in metastable β-Ti alloys [126,131,136], i.e., the interstitial oxygen acts as a strong β-stabilizing element in metastable β-Ti alloys. Doping 0.3 wt.% oxygen combined with grain refinement was successfully employed by Chong et al. to substantially improve the yield strength of Ti-12Mo-0.3O to 826 MPa while maintaining a high strain hardening ability and high uniform elongation [135]. The beneficial role of O interstitial strengthening is also reported in Ti-32Nb [118], Ti-38Nb [118,129], and Ti-20V [127]. However, oxygen is excluded by the calculation of electron parameters $\overline{Bo}$, $\overline{Md}$, and $\overline{e/a}$, while it is treated as an α-stabilizer in calculating the $[Mo]_{eq}$, meaning that the β-stabilizing effect of interstitial oxygen is not considered in the current semi-empirical alloy design approaches. So do the neutral elements Zr and Sn. Consequently, the current *d*-electron theory, $[Mo]_{eq}$, and electron-to-atom ratio approach need to be modified to fully harness the benefits of the β-stabilizing effect of oxygen, Zr, and Sn, and their interaction with other β-stabilizers.

4.2. Precipitation Strengthening

4.2.1. α Precipitation Strengthening

The yield strength can also be enhanced by developing TRIP/TWIP Ti alloys from the single β phase alloys to β + α and β + ω dual-phase alloys, which can be achieved by utilizing equiaxed α phase or nanoscale ω phase precipitation to strengthen the least stable β matrix. The yield strength (760 MPa) of 20% α strengthened Ti-7Cr-1.5Sn dual-phase alloy is 200 MPa higher than that of the Ti-8.5Cr-1.5Sn single β phase alloy while maintaining the TRIP/TWIP effects [59]. A transition from TRIP to TRIP/TWIP in Ti-10V-2Fe-3Al accompanied by remarkably enhanced yield strength was achieved by precipitating the 20% α phase [15]. Simultaneously enhanced yield strength, ultimate tensile strength, and ductility were observed in a 4 vol.% α containing α + β dual-phase Ti-3Mo-3Cr-2Fe-2Al TRIP/TWIP alloy as compared to its single-phase counterpart [17]. The precipitation of the α phase leads to solute-atom partitioning, enriching the β matrix with β-stabilizers and thus enhancing its phase stability, which results in a transition of deformation mechanism from TRIP to TWIP or even the complete suppression of the TRIP/TWIP effect. It appears that a small fraction of no more than 20 vol.% α should be ensured to maintain the TRIP/TWIP effects in α + β dual-phase Ti alloys [20,98,137,138]. The volume fraction of α precipitates and the resultant transition of deformation mode in α + β dual-phase TRIP/TWIP Ti alloys can be guided by coupling the Calphad calculation and $\overline{Bo}$-$\overline{Md}$ diagram [15,59]. The α precipitation strengthening opens a new branch of TRIP/TWIP Ti alloy development from single β phase alloys to α + β dual phase alloys.

4.2.2. ω Precipitation Strengthening

Controlling the development of ω phase has also been shown to be quite effective in increasing the yield strength of TRIP/TWIP Ti alloys while reserving their promising strain hardening, leading to the development of ω strengthened β + ω dual-phase TRIP/TWIP Ti alloys [18,99]. Sun et al. [99] conducted low-temperature short-time aging (150 °C for 60 s) to control the development of the isothermal ω phase in Ti-12Mo without causing any discernible compositional partitioning. This method takes full advantage of the precipitation hardening of the ω phase while minimizing its harmful effect on suppressing stress-induced martensitic transformation and deformation twinning. The result was a substantial increase in yield strength from 480 MPa to 730 MPa while maintaining the original high ductility. Low-temperature short-time aging (200 °C for 60 s) combined with grain refinement was employed by Qian et al. [18] to achieve high yield strength as high

as 990 MPa in Ti-12Mo without significantly sacrificing the ductility. Enhanced uniform elongation in the Ti-15Mo TWIP alloy was achieved by Min et al. through coupling pre-strain-induced twins and isothermal ω (ω_{iso}) precipitation, as compared to the counterpart with only ω_{iso} precipitation [132,139,140]. These works have highlighted the potential of tuning the ω phase precipitation to enhance the mechanical properties of TRIP/TWIP Ti alloys.

It is worth mentioning that the athermal ω (ω_{ath}) phase formed during quenching is not harmful to the mechanical properties of TRIP/TWIP Ti alloys, contrary to the isothermal ω phase. It is reported that the ω_{ath} disappeared after the formation of stress-induced martensite and deformation twinning, which is believed to be reversed back to the parent β phase during deformation [7,8,93]. The excellent combination of high yield strength of 870 MPa, ultimate tensile strength of 1092 MPa, and excellent ductility with a fracture elongation of 41% observed in Ti-4Mo-3Cr-1Fe is likely related to the dynamic ω_{ath}-to-β reversion during tensile deformation, which promotes the formation of stress-induced nano-scale hierarchical twinning structures [7].

The ω_{ath}-to-β reversion ability during deformation makes it possible to tune the deformation mechanisms and mechanical properties of TRIP/TWIP Ti alloys by regulating the development of ω_{ath}. This can be realized by low-temperature short-time aging [5,18,99] and room-temperature aging [5,51]. Accordingly, substantially increased yield strength without obviously sacrificing ductility or even enhanced ductility was achieved in Ti-12Mo, Ti-10V-2Fe-3Al, and Ti-15Nb-5Zr-4Sn-1Fe [5,18,51,99]. Especially, a high yield strength of 683 MPa, which is comparable to most of the TRIP/TWIP Ti alloys, was reported in a TRIP Ti-15Nb-5Zr-4Sn-1Fe TRIP Ti alloy after regulating the ω_{ath} by nature aging [51]. These results demonstrate a new opportunity to enhance the mechanical properties of TRIP/TWIP Ti alloys via engineering the ω_{ath}. Future efforts may be dedicated to revealing the evolution of ω_{ath} during aging and its influence on the deformation mechanisms and mechanical properties of TRIP/TWIP Ti alloys.

4.3. Grain Refinement Strengthening

The role of grain refinement strengthening in increasing the yield strength of TRIP/TWIP Ti alloys has received little attention. This might be attributed to the fact that the critical resolved shear stress for stress-induced martensitic phase transformation and deformation twinning is not very sensitive to changes in grain size [141–143]. A higher yield strength was observed in coarser-grained TRIP Ti alloys [144–146]. Accordingly, the impact of grain refinement on the yield strength of TRIP/TWIP Ti alloys is limited. It is challenging to refine the grain size of metastable β-Ti alloys to the ultrafine grain scale after undergoing severe plastic deformation. This difficulty is related to the rapid recrystallization and grain growth kinetics during the annealing of Ti alloys above the β transus temperatures [135,142].

Chong et al. [135] demonstrate that significantly refining the grain size from 50 μm to 4.5 μm in Ti-12Mo only slightly increased the yield strength by 43 MPa. A similar result has also been reported in Ti-13.3Nb-4.6Mo (at.%) [130]. This is because substantial grain refinement promotes the occurrence of stress-induced martensitic phase transformation, leading to a reduction in the ultimate tensile strength and ductility. However, combining grain refinement with other strengthening methods, such as α phase precipitation [17], ω phase precipitation [18], and oxygen addition [26], has shown the potential to significantly increase the yield strength while maintaining high ductility and a high work-hardening rate. Therefore, the combination of grain refinement with other strengthening methods is worthy of further research and exploration.

5. Summary

The past decade has witnessed the vigorous development of TRIP/TWIP Ti alloys. Compositional design, deformation mechanisms, and mechanical properties of TRIP/TWIP Ti alloys are hot spots in the field of Ti alloy research. After reviewing the deformation

mechanisms and its correlation with mechanical properties, the compositional design strategies, and the recent development of TRIP/TWIP Ti alloys with a focus on enhancing their yield strength, some suggestions regarding the in-depth understanding of TRIP/TWIP Ti alloy for future research are recommended as follows:

(1) Considering the effect of solid solution strengthening atoms and their complex interactions on changing the stability of the β phase and TRIP/TWIP behaviors. On this basis, the boundaries are modified, and the accuracy of the existing semi-empirical compositional design methods is improved. Consequently, optimized deformation behaviors and correlating mechanical properties of TRIP/TWIP can be manipulated by tailoring chemical compositions.

(2) The stress-induced martensitic transformation and deformation twinning of TRIP/TWIP Ti alloys and their interactions are quite complex and heterogeneous, setting difficulties in investigating them using ex situ techniques. In situ methods, such as in situ synchrotron X-ray diffraction (SXRD), in situ electron backscattered diffraction (EBSD), and in situ transmission electron microscopy (TEM), are highly plausible to study the microstructure evolution during static/dynamic loading. This detailed understanding of the interactions among the multiple deformation modes and their correlation with the mechanical properties will lay the foundation for the development of new TRIP/TWIP Ti alloys.

(3) Addressing the limitation of relatively low yield strength in TRIP/TWIP Ti alloys is crucial to broaden their potential engineering applications. Previous research has mainly focused on designing new TRIP/TWIP Ti alloys and understanding their deformation mechanisms, but there has been a notable gap in exploring enhancing the yield strength of these alloys. Oxygen interstitial solid solution strengthening and ω phase strengthening are promising approaches to improve yield strength without compromising the high ductility and high strain hardening rate in TRIP/TWIP Ti alloys. Future research can delve into the implementation and mechanisms of these strengthening methods.

Author Contributions: Conceptualization, W.X., X.Z. and C.M.; writing—original draft preparation, Y.F., Y.G. and W.J.; writing—review and editing, Y.F. and W.X.; supervision, W.X., X.Z. and C.M.; project administration, W.X. and C.M.; funding acquisition, W.X. All authors have read and agreed to the published version of the manuscript.

Funding: This work was financially supported by the National Natural Science Foundation of China (No. 51671012) and the Youth Talent Support Program of Beihang University.

Data Availability Statement: No new data were created in this study. Data sharing does not apply to this article.

Conflicts of Interest: The authors declare no conflict of interest.

References

1. Banerjee, D.; Williams, J.C. Perspectives on titanium science and technology. *Acta Mater.* **2013**, *61*, 844–879. [CrossRef]
2. Devaraj, A.; Joshi, V.V.; Srivastava, A.; Manandhar, S.; Moxson, V.; Duz, V.A.; Lavender, C. A low-cost hierarchical nanostructured beta-titanium alloy with high strength. *Nat. Commun.* **2016**, *7*, 11176. [CrossRef] [PubMed]
3. Cotton, J.D.; Briggs, R.D.; Boyer, R.R.; Tamirisakandala, S.; Russo, P.; Shchetnikov, N.; Fanning, J.C. State of the art in beta titanium alloys for airframe applications. *Miner. Met. Mater. Ser.* **2015**, *67*, 1281–1303. [CrossRef]
4. Brozek, C.; Sun, F.; Vermaut, P.; Millet, Y.; Lenain, A.; Embury, D.; Jacques, P.J.; Prima, F. A β-titanium alloy with extra high strain-hardening rate: Design and mechanical properties. *Scr. Mater.* **2016**, *114*, 60–64. [CrossRef]
5. Ellyson, B.; Klemm-Toole, J.; Clarke, K.; Field, R.; Kaufman, M.; Clarke, A. Tuning the strength and ductility balance of a TRIP titanium alloy. *Scr. Mater.* **2021**, *194*, 113641. [CrossRef]
6. Sun, F.; Zhang, J.Y.; Marteleur, M.; Gloriant, T.; Vermaut, P.; Laillé, D.; Castany, P.; Curfs, C.; Jacques, P.J.; Prima, F. Investigation of early stage deformation mechanisms in a metastable β titanium alloy showing combined twinning-induced plasticity and transformation-induced plasticity effects. *Acta Mater.* **2013**, *61*, 6406–6417. [CrossRef]

7. Ren, L.; Xiao, W.; Kent, D.; Wan, M.; Ma, C.; Zhou, L. Simultaneously enhanced strength and ductility in a metastable β-Ti alloy by stress-induced hierarchical twin structure. *Scr. Mater.* **2020**, *184*, 6–11. [CrossRef]
8. Fu, Y.; Xiao, W.; Kent, D.; Dargusch, M.S.; Wang, J.; Zhao, X.; Ma, C. Ultrahigh strain hardening in a transformation-induced plasticity and twinning-induced plasticity titanium alloy. *Scr. Mater.* **2020**, *187*, 285–290. [CrossRef]
9. Zhang, Y.; Song, R.; Wang, Y.; Cai, C.; Wang, H.; Wang, K. C-modified stacking-fault networks inducing the excellent strength-plasticity combinations of medium manganese steel by simple two-stage warm rolling without annealing. *Scr. Mater.* **2023**, *229*, 115372. [CrossRef]
10. Zhi, H.; Li, J.; Li, W.; Elkot, M.; Antonov, S.; Zhang, H.; Lai, M. Simultaneously enhancing strength-ductility synergy and strain hardenability via Si-alloying in medium-Al FeMnAlC lightweight steels. *Acta Mater.* **2023**, *245*, 118611. [CrossRef]
11. Gao, J.; Jiang, S.; Zhang, H.; Huang, Y.; Guan, D.; Xu, Y.; Guan, S.; Bendersky, L.A.; Davydov, A.V.; Wu, Y.; et al. Facile route to bulk ultrafine-grain steels for high strength and ductility. *Nature* **2021**, *590*, 262–267. [CrossRef] [PubMed]
12. Marteleur, M.; Sun, F.; Gloriant, T.; Vermaut, P.; Jacques, P.J.; Prima, F. On the design of new β-metastable titanium alloys with improved work hardening rate thanks to simultaneous TRIP and TWIP effects. *Scr. Mater.* **2012**, *66*, 749–752. [CrossRef]
13. Sadeghpour, S.; Abbasi, S.M.; Morakabati, M.; Kisko, A.; Karjalainen, L.P.; Porter, D.A. A new multi-element beta titanium alloy with a high yield strength exhibiting transformation and twinning induced plasticity effects. *Scr. Mater.* **2018**, *145*, 104–108. [CrossRef]
14. Ren, L.; Xiao, W.; Ma, C.; Zheng, R.; Zhou, L. Development of a high strength and high ductility near β-Ti alloy with twinning induced plasticity effect. *Scr. Mater.* **2018**, *156*, 47–50. [CrossRef]
15. Danard, Y.; Poulain, R.; Garcia, M.; Guillou, R.; Thiaudière, D.; Mantri, S.; Banerjee, R.; Sun, F.; Prima, F. Microstructure design and in-situ investigation of TRIP/TWIP effects in a forged dual-phase Ti-10V-2Fe-3Al alloy. *Materialia* **2019**, *8*, 100507. [CrossRef]
16. Ahmed, M.; Wexler, D.; Casillas, G.; Ivasishin, O.M.; Pereloma, E.V. The influence of β phase stability on deformation mode and compressive mechanical properties of Ti-10V-3Fe-3Al alloy. *Acta Mater.* **2015**, *84*, 124–135. [CrossRef]
17. Lee, S.W.; Park, C.H.; Hong, J.-K.; Yeom, J.-T. Development of sub-grained α+β Ti alloy with high yield strength showing twinning- and transformation-induced plasticity. *J. Alloys Compd.* **2020**, *813*, 152102. [CrossRef]
18. Qian, B.; Mantri, S.A.; Dasari, S.; Zhang, J.; Lilensten, L.; Sun, F.; Vermaut, P.; Banerjee, R.; Prima, F. Mechanisms underlying enhanced strength-ductility combinations in TRIP/TWIP Ti-12Mo alloy engineered via isothermal omega precipitation. *Acta Mater.* **2023**, *245*, 118619. [CrossRef]
19. Lee, S.; Park, C.; Hong, J.; Yeom, J.-t. The role of nano-domains in {1–011} twinned martensite in metastable titanium alloys. *Sci. Rep.* **2018**, *8*, 11914. [CrossRef]
20. Lee, S.W.; Oh, J.M.; Park, C.H.; Hong, J.-K.; Yeom, J.-T. Deformation mechanism of metastable titanium alloy showing stress-induced α′-Martensitic transformation. *J. Alloys Compd.* **2019**, *782*, 427–432. [CrossRef]
21. Kuan, T.S.; Ahrens, R.R.; Sass, S.L. The stress-induced omega phase transformation in Ti-V alloys. *Metall. Trans. A* **1974**, *6A*, 1767–1774. [CrossRef]
22. Zhao, X.; Niinomi, M.; Nakai, M. Relationship between various deformation-induced products and mechanical properties in metastable Ti-30Zr-Mo alloys for biomedical applications. *J. Mech. Behav. Biomed. Mater.* **2011**, *4*, 2009–2016. [CrossRef] [PubMed]
23. Pinilla Ducreux, C.I.; Saleh, A.A.; Gazder, A.A.; Pereloma, E.V. An in-situ neutron diffraction investigation of martensitic transformation in a metastable β Ti-10V-2Fe-3Al alloy during uniaxial tension. *J. Alloys Compd.* **2021**, *869*, 159301. [CrossRef]
24. Castany, P.; Ramarolahy, A.; Prima, F.; Laheurte, P.; Curfs, C.; Gloriant, T. In situ synchrotron X-ray diffraction study of the martensitic transformation in superelastic Ti-24Nb-0.5N and Ti-24Nb-0.5O alloys. *Acta Mater.* **2015**, *88*, 102–111. [CrossRef]
25. Song, B.; Xiao, W.; Ma, C.; Zhou, L. Tuning the strength and ductility of near β titanium alloy Ti-5321 by ω and O′ intermediate phases via low-temperature aging. *Mater. Sci. Eng. A* **2022**, *855*, 143919. [CrossRef]
26. Bortolan, C.C.; Campanelli, L.C.; Paternoster, C.; Giguère, N.; Brodusch, N.; Bolfarini, C.; Gauvin, R.; Mengucci, P.; Barucca, G.; Mantovani, D. Effect of oxygen content on the mechanical properties and plastic deformation mechanisms in the TWIP/TRIP Ti-12Mo alloy. *Mater. Sci. Eng. A* **2021**, *817*, 141346. [CrossRef]
27. An, X.; Jiang, W.; Ni, S.; Chen, Z.; Wang, Z.; Song, M. Origin of {332} <113> twinning and twin-twin intersections in a shock load metastable β Ti-12Mo alloy. *Mater. Charact.* **2023**, *197*, 112674. [CrossRef]
28. Liu, H.; Niinomi, M.; Nakai, M.; Cho, K.; Fujii, H. Deformation-induced ω-phase transformation in a β-type titanium alloy during tensile deformation. *Scr. Mater.* **2017**, *130*, 27–31. [CrossRef]
29. Chen, K.; Fan, Q.; Xu, S.; Yao, J.; Yang, L.; Yuan, J.; Gong, H.; Zhang, H.; Cheng, X. Excellent strength-ductility balance of a titanium alloy via controlling stress-induced ω transformation assisted by α-β hybrid structure. *Mater. Sci. Eng. A* **2022**, *853*, 143739. [CrossRef]
30. Wang, X.L.; Li, L.; Mei, W.; Wang, W.L.; Sun, J. Dependence of stress-induced omega transition and mechanical twinning on phase stability in metastable β Ti-V alloys. *Mater. Charact.* **2015**, *107*, 149–155. [CrossRef]
31. Zhao, X.L.; Li, L.; Niinomi, M.; Nakai, M.; Zhang, D.L.; Suryanarayana, C. Metastable Zr-Nb alloys for spinal fixation rods with tunable Young's modulus and low magnetic resonance susceptibility. *Acta Biomater.* **2017**, *62*, 372–384. [CrossRef] [PubMed]
32. Sadeghpour, S.; Abbasi, S.M.; Morakabati, M.; Kisko, A.; Karjalainen, L.P.; Porter, D.A. On the compressive deformation behavior of new beta titanium alloys designed by d-electron method. *J. Alloys Compd.* **2018**, *746*, 206–217. [CrossRef]

33. Shin, S.; Zhu, C.; Vecchio, K.S. Observations on {332}<113> twinning-induced softening in Ti-Nb Gum metal. *Mater. Sci. Eng. A* **2018**, *724*, 189–198. [CrossRef]
34. Lu, H.; Ji, P.; Li, B.; Ma, W.; Chen, B.; Zhang, X.; Zhang, X.; Ma, M.; Liu, R. Mechanical properties and deformation mechanism of a novel metastable β-type Ti-4V-2Mo-2Fe alloy. *Mater. Sci. Eng. A* **2022**, *848*, 143376. [CrossRef]
35. Qi, L.; Qiao, X.; Huang, L.; Huang, X.; Zhao, X. Effect of structural stability on the stress induced martensitic transformation in Ti-10V-2Fe-3Al alloy. *Mater. Sci. Eng. A* **2019**, *756*, 381–388. [CrossRef]
36. Xue, Q.; Ma, Y.J.; Lei, J.F.; Yang, R.; Wang, C. Mechanical properties and deformation mechanisms of Ti-3Al-5Mo-4.5 V alloy with varied β phase stability. *J. Mater. Sci. Technol.* **2018**, *34*, 2507–2514. [CrossRef]
37. Catanio Bortolan, C.; Contri Campanelli, L.; Mengucci, P.; Barucca, G.; Giguère, N.; Brodusch, N.; Paternoster, C.; Bolfarini, C.; Gauvin, R.; Mantovani, D. Development of Ti-Mo-Fe alloys combining different plastic deformation mechanisms for improved strength-ductility trade-off and high work hardening rate. *J. Alloys Compd.* **2022**, *925*, 166757. [CrossRef]
38. Min, X.; Chen, X.; Emura, S.; Tsuchiya, K. Mechanism of twinning-induced plasticity in β-type Ti-15Mo alloy. *Scr. Mater.* **2013**, *69*, 393–396. [CrossRef]
39. Ma, X.; Li, F.; Cao, J.; Li, J.; Sun, Z.; Zhu, G.; Zhou, S. Strain rate effects on tensile deformation behaviors of Ti-10V-2Fe-3Al alloy undergoing stress-induced martensitic transformation. *Mater. Sci. Eng. A* **2018**, *710*, 1–9. [CrossRef]
40. Zhang, J.; Sun, F.; Chen, Z.; Yang, Y.; Shen, B.; Li, J.; Prima, F. Strong and ductile beta Ti-18Zr-13Mo alloy with multimodal twinning. *Mater. Res. Lett.* **2019**, *7*, 251–257. [CrossRef]
41. Zhao, G.-H.; Xu, X.; Dye, D.; Rivera-Díaz-del-Castillo, P.E.J. Microstructural evolution and strain-hardening in TWIP Ti alloys. *Acta Mater.* **2020**, *183*, 155–164. [CrossRef]
42. Yao, K.; Min, X. Static and dynamic Hall-Petch relations in {332}<113> TWIP Ti-15Mo alloy. *Mater. Sci. Eng. A* **2021**, *827*, 142044. [CrossRef]
43. Castany, P.; Gloriant, T.; Sun, F.; Prima, F. Design of strain-transformable titanium alloys. *C. R. Phys.* **2018**, *19*, 710–720. [CrossRef]
44. Gao, J.J.; Castany, P.; Gloriant, T. Complex multi-step martensitic twinning process during plastic deformation of the superelastic Ti-20Zr-3Mo-3Sn alloy. *Acta Mater.* **2022**, *236*, 118140. [CrossRef]
45. Zhu, C.; Zhang, X.-y.; Li, C.; Liu, C.; Zhou, K. A strengthening strategy for metastable β titanium alloys: Synergy effect of primary α phase and β phase stability. *Mater. Sci. Eng. A* **2022**, *852*, 143736. [CrossRef]
46. Min, X.; Emura, S.; Chen, X.; Zhou, X.; Tsuzaki, K.; Tsuchiya, K. Deformation microstructural evolution and strain hardening of differently oriented grains in twinning-induced plasticity β titanium alloy. *Mater. Sci. Eng. A* **2016**, *659*, 1–11. [CrossRef]
47. Zhang, J.; Qian, B.; Lin, W.; Zhang, P.; Wu, Y.; Fu, Y.; Fan, Y.; Chen, Z.; Cheng, J.; Li, J.; et al. Compressive deformation-induced hierarchical microstructure in a TWIP β Ti-alloy. *J. Mater. Sci. Technol.* **2022**, *112*, 130–137. [CrossRef]
48. Zhang, J.; Fu, Y.; Wu, Y.; Qian, B.; Chen, Z.; Inoue, A.; Wu, Y.; Yang, Y.; Sun, F.; Li, J.; et al. Hierarchical {332}<113> twinning in a metastable β Ti-alloy showing tolerance to strain localization. *Mater. Res. Lett.* **2020**, *8*, 247–253. [CrossRef]
49. Qian, B.; Zhang, J.; Fu, Y.; Sun, F.; Wu, Y.; Cheng, J.; Vermaut, P.; Prima, F. In-situ microstructural investigations of the TRIP-to-TWIP evolution in Ti-Mo-Zr alloys as a function of Zr concentration. *J. Mater. Sci. Technol.* **2021**, *65*, 228–237. [CrossRef]
50. Zhao, G.; Li, X.; Petrinic, N. Materials information and mechanical response of TRIP/TWIP Ti alloys. *NJP Comput. Mater.* **2021**, *7*, 91. [CrossRef]
51. Fu, Y.; Xiao, W.; Kent, D.; Rong, J.; Zhao, X.; Ma, C. Natural aging of a metastable β-type titanium alloy to simultaneously enhance yield strength and uniform elongation. *Scr. Mater.* **2023**, *234*, 115569. [CrossRef]
52. Zhang, Z.; Jiang, Z.; Xie, Y.; Chan, S.L.I.; Liang, J.; Wang, J. Multiple deformation mechanisms induced by pre-twinning in CoCrFeNi high entropy alloy. *Scr. Mater.* **2022**, *207*, 114266. [CrossRef]
53. Jing, T.; Dong, S.; Shen, L.; Peng, H.; Wen, Y. Achieving strength-ductility synergy in nanotwinned steels prepared by cryogenic deformation. *Mater. Charact.* **2023**, *195*, 112512. [CrossRef]
54. Zhao, G.; Xu, X.; Dye, D.; Rivera-Díaz-del-Castillo, P.E.J.; Petrinic, N. Facile route to implement transformation strengthening in titanium alloys. *Scr. Mater.* **2022**, *208*, 114362. [CrossRef]
55. Morinaga, M.; Yukawa, H. Alloy design with the aid of molecular orbital method. *Bull. Mater. Sci.* **1997**, *20*, 805–815. [CrossRef]
56. Abdel-Hady, M.; Hinoshita, K.; Morinaga, M. General approach to phase stability and elastic properties of β-type Ti-alloys using electronic parameters. *Scr. Mater.* **2006**, *55*, 477–480. [CrossRef]
57. Sun, F.; Zhang, J.Y.; Marteleur, M.; Brozek, C.; Rauch, E.F.; Veron, M.; Vermaut, P.; Jacques, P.J.; Prima, F. A new titanium alloy with a combination of high strength, high strain hardening and improved ductility. *Scr. Mater.* **2015**, *94*, 17–20. [CrossRef]
58. Chen, K.; Fan, Q.; Yao, J.; Yang, L.; Xu, S.; Lei, W.; Wang, D.; Yuan, J.; Gong, H.; Cheng, X. Composition design of a novel Ti-6Mo-3.5Cr-1Zr alloy with high-strength and ultrahigh-ductility. *J. Mater. Sci. Technol.* **2022**, *131*, 276–286. [CrossRef]
59. Lilensten, L.; Danard, Y.; Poulain, R.; Guillou, R.; Joubert, J.M.; Perrière, L.; Vermaut, P.; Thiaudière, D.; Prima, F. From single phase to dual-phase TRIP-TWIP titanium alloys: Design approach and properties. *Materialia* **2020**, *12*, 100700. [CrossRef]
60. Castany, P.; Yang, Y.; Bertrand, E.; Gloriant, T. Reversion of a parent {130}<310>$_{\alpha''}$ martensitic twinning system at the origin of {332}<113>$_{\beta}$ twins observed in metastable β titanium alloys. *Phys. Rev. Lett.* **2016**, *117*, 245501. [CrossRef]
61. Cho, K.; Morioka, R.; Harjo, S.; Kawasaki, T.; Yasuda, H.Y. Study on formation mechanism of {332}<113> deformation twinning in metastable β-type Ti alloy focusing on stress-induced α″ martensite phase. *Scr. Mater.* **2020**, *177*, 106–111. [CrossRef]

62. Chen, N.; Molina-Aldareguia, J.M.; Kou, H.; Qiang, F.; Wu, Z.; Li, J. Reversion martensitic phase transformation induced {3 3 2}<1 1 3> twinning in metastable β-Ti alloys. *Mater. Lett.* **2020**, *272*, 127883. [CrossRef]
63. Xiao, J.F.; He, B.B.; Tan, C.W. Effect of martensite on {332} twinning formation in a metastable beta titanium alloy. *J. Alloys Compd.* **2022**, *895*, 162598. [CrossRef]
64. Gao, J.; Huang, Y.; Hu, X.; Wang, S.; Rainforth, W.M.; Todd, I.; Zhu, Q. An alternative formation mechanism of {332}BCC twinning in metastable body-centered-cubic high entropy alloy. *Scr. Mater.* **2022**, *217*, 114770. [CrossRef]
65. Tobe, H.; Kim, H.Y.; Inamura, T.; Hosoda, H.; Miyazaki, S. Origin of {332} twinning in metastable β-Ti alloys. *Acta Mater.* **2014**, *64*, 345–355. [CrossRef]
66. Tane, M.; Nakano, T.; Kuramoto, S.; Hara, M.; Niinomi, M.; Takesue, N.; Yano, T.; Nakajima, H. Low Young's modulus in Ti–Nb–Ta–Zr–O alloys: Cold working and oxygen effects. *Acta Mater.* **2011**, *59*, 6975–6988. [CrossRef]
67. Zhang, J.Y.; Li, J.S.; Chen, Z.; Meng, Q.K.; Sun, F.; Shen, B.L. Microstructural evolution of a ductile metastable β titanium alloy with combined TRIP/TWIP effects. *J. Alloys Compd.* **2017**, *699*, 775–782. [CrossRef]
68. Danard, Y.; Martin, G.; Lilensten, L.; Sun, F.; Seret, A.; Poulain, R.; Mantri, S.; Guillou, R.; Thiaudière, D.; Freiherr von Thüngen, I.; et al. Accommodation mechanisms in strain-transformable titanium alloys. *Mater. Sci. Eng. A* **2021**, *819*, 141437. [CrossRef]
69. Bertrand, E.; Castany, P.; Yang, Y.; Menou, E.; Couturier, L.; Gloriant, T. Origin of {112} < 111 > antitwinning in a Ti-24Nb-4Zr-8Sn superelastic single crystal. *J. Mater. Sci.* **2022**, *57*, 7327–7342. [CrossRef]
70. Yang, Y.; Castany, P.; Bertrand, E.; Cornen, M.; Lin, J.X.; Gloriant, T. Stress release-induced interfacial twin boundary ω phase formation in a β type Ti-based single crystal displaying stress-induced α″ martensitic transformation. *Acta Mater.* **2018**, *149*, 97–107. [CrossRef]
71. Zhang, D.C.; Xue, Q.; Lei, J.F.; Ma, Y.J.; Yang, R.; Wang, C. Influence of Grain Size on Mechanical Responses in Beta Ti-12Mo Alloy Demonstrating Concurrent Twinning-Induced Plasticity/Transformation-induced Plasticity Effects. *Metall. Mater. Trans. A* **2018**, *49*, 3161–3166. [CrossRef]
72. Zhang, C.; Liu, S.; Zhang, J.; Zhang, D.; Kuang, J.; Bao, X.; Liu, G.; Sun, J. Trifunctional nanoprecipitates ductilize and toughen a strong laminated metastable titanium alloy. *Nat. Commun.* **2023**, *14*, 1397. [CrossRef] [PubMed]
73. Ma, X.; Li, F.; Sun, Z.; Hou, J.; Fang, X.; Zhu, Y.; Koch, C.C. Achieving Gradient Martensite Structure and Enhanced Mechanical Properties in a Metastable β Titanium Alloy. *Metall. Mater. Trans. A* **2019**, *50*, 2126–2138. [CrossRef]
74. Zhao, X.; Zhu, R.; Song, W.; Meng, L.; Niinomi, M.; Nakano, T.; Jia, N.; Zhang, D. A strategy to regulate the yield ratio of a metastable high Zr-containing β titanium alloy: Synergistic effects of the β domain, β stability and β/α interfaces by varying the α phase content. *J. Alloys Compd.* **2023**, *952*, 170024. [CrossRef]
75. Sang, Z.; Wang, L.; Chen, J.; Fan, Q.; Zhou, S.; Tao, L.; Wu, Y.; Peng, X.; Zhou, Z.; Yao, J. Excellent strength-ductility balance via controlling stress-induced α′ martensite transformation of Ti422 alloy. *Mater. Sci. Eng. A* **2023**, *884*, 145558. [CrossRef]
76. Oh, J.M.; Park, C.H.; Yeom, J.-T.; Hong, J.-K.; Kang, N.; Lee, S.W. High strength and ductility in low-cost Ti-Al-Fe-Mn alloy exhibiting transformation-induced plasticity. *Mater. Sci. Eng. A* **2020**, *772*, 138813. [CrossRef]
77. Eleti, R.R.; Klimova, M.; Tikhonovsky, M.; Stepanov, N.; Zherebtsov, S. Exceptionally high strain-hardening and ductility due to transformation induced plasticity effect in Ti-rich high-entropy alloys. *Sci. Rep.* **2020**, *10*, 13293. [CrossRef]
78. Wen, X.; Zhu, L.; Naeem, M.; Huang, H.; Jiang, S.; Wang, H.; Liu, X.; Zhang, X.; Wang, X.-L.; Wu, Y.; et al. Strong work-hardenable body-centered-cubic high-entropy alloys at cryogenic temperature. *Scr. Mater.* **2023**, *231*, 115434. [CrossRef]
79. Bönisch, M.; Waitz, T.; Calin, M.; Skrotzki, W.; Eckert, J. Tailoring the Bain strain of martensitic transformations in TiNb alloys by controlling the Nb content. *Inter. J. Plast.* **2016**, *85*, 190–202. [CrossRef]
80. Bönisch, M.; Calin, M.; Giebeler, L.; Helth, A.; Gebert, A.; Skrotzki, W.; Eckert, J. Composition-dependent magnitude of atomic shuffles in Ti–Nb martensites. *J. Appl. Crystall.* **2014**, *47*, 1374–1379. [CrossRef]
81. Wang, X.D.; Lou, H.B.; Ståhl, K.; Bednarcik, J.; Franz, H.; Jiang, J.Z. Tensile behavior of orthorhombic α″-titanium alloy studied by in situ X-ray diffraction. *Mater. Sci. Eng. A* **2010**, *527*, 6596–6600. [CrossRef]
82. Yan, X.; Xu, X.; Zhao, Y.; Zhou, Y.; Wei, L.; Wu, Z.; Yu, Y.; Wu, C. Achieving low elastic modulus, excellent work hardening and high corrosion resistance in Ti-6Al-4V-5.6Cu alloy. *J. Alloys Compd.* **2023**, *959*, 170582. [CrossRef]
83. Rastogi, A.; Sarkar, R.; Neelakantan, S. Transitions among martensitic phases during continuous deformation in metastable β Ti-10V-2Fe-3Al alloy. *J. Alloys Compd.* **2023**, *964*, 171320. [CrossRef]
84. Chung, C.-C.; Wang, S.-W.; Chen, Y.-C.; Ju, C.-P.; Chern Lin, J.-H. Effect of cold rolling on structure and tensile properties of cast Ti–7.5Mo alloy. *Mater. Sci. Eng. A* **2015**, *631*, 52–66. [CrossRef]
85. Lai, M.J.; Li, T.; Raabe, D. ω phase acts as a switch between dislocation channeling and joint twinning- and transformation-induced plasticity in a metastable β titanium alloy. *Acta Mater.* **2018**, *151*, 67–77. [CrossRef]
86. Ballor, J.; Li, T.; Prima, F.; Boehlert, C.J.; Devaraj, A. A review of the metastable omega phase in beta titanium alloys: The phase transformation mechanisms and its effect on mechanical properties. *Inter. Mater. Rev.* **2022**, *68*, 26–45. [CrossRef]
87. Nag, S.; Devaraj, A.; Srinivasan, R.; Williams, R.E.; Gupta, N.; Viswanathan, G.B.; Tiley, J.S.; Banerjee, S.; Srinivasan, S.G.; Fraser, H.L.; et al. Novel mixed-mode phase transition involving a composition-dependent displacive component. *Phys. Rev. Lett.* **2011**, *106*, 245701. [CrossRef]
88. Zhang, J.Y.; Chen, G.F.; Fu, Y.Y.; Fan, Y.; Chen, Z.; Xu, J.; Chang, H.; Zhang, Z.H.; Zhou, J.; Sun, Z.; et al. Strengthening strain-transformable β Ti-alloy via multi-phase nanostructuration. *J. Alloys Compd.* **2019**, *799*, 389–397. [CrossRef]

89. Lai, M.J.; Li, T.; Yan, F.K.; Li, J.S.; Raabe, D. Revisiting ω phase embrittlement in metastable β titanium alloys: Role of elemental partitioning. *Scr. Mater.* **2021**, *193*, 38–42. [CrossRef]
90. Mantri, S.A.; Choudhuri, D.; Alam, T.; Ageh, V.; Sun, F.; Prima, F.; Banerjee, R. Change in the deformation mode resulting from beta-omega compositional partitioning in a Ti Mo alloy: Room versus elevated temperature. *Scr. Mater.* **2017**, *130*, 69–73. [CrossRef]
91. Gao, J.; Knowles, A.J.; Guan, D.; Rainforth, W.M. ω phase strengthened 1.2GPa metastable β titanium alloy with high ductility. *Scr. Mater.* **2019**, *162*, 77–81. [CrossRef]
92. Chen, W.; Li, K.; Yu, G.; Ren, J.; Zha, Y.; Sun, J. Deformation twinning-induced single-variant ω-plates in metastable β-Ti alloys containing athermal ω-precipitates. *J. Mater. Sci.* **2021**, *56*, 7710–7726. [CrossRef]
93. Xiao, J.F.; Nie, Z.H.; Tan, C.W.; Zhou, G.; Chen, R.; Li, M.R.; Yu, X.D.; Zhao, X.C.; Hui, S.X.; Ye, W.J.; et al. Effect of reverse β-to-ω transformation on twinning and martensitic transformation in a metastable β titanium alloy. *Mater. Sci. Eng. A* **2019**, *759*, 680–687. [CrossRef]
94. Chen, Q.-J.; Ma, S.-Y.; Wang, S.-Q. The assisting and stabilizing role played by ω phase during the 112111β twinning in Ti-Mo alloys: A first-principles insight. *J. Mater. Sci. Technol.* **2021**, *80*, 163–170. [CrossRef]
95. Wu, S.Q.; Ping, D.H.; Yamabe-Mitarai, Y.; Xiao, W.L.; Yang, Y.; Hu, Q.M.; Li, G.P.; Yang, R. {112}<111> Twinning during ω to body-centered cubic transition. *Acta Mater.* **2014**, *62*, 122–128. [CrossRef]
96. Wang, W.; Zhang, X.; Mei, W.; Sun, J. Role of omega phase evolution in plastic deformation of twinning-induced plasticity β Ti–12V–2Fe–1Al alloy. *Mater. Des.* **2020**, *186*, 108282. [CrossRef]
97. Chen, W.; Cao, S.; Kou, W.; Zhang, J.; Wang, Y.; Zha, Y.; Pan, Y.; Hu, Q.; Sun, Q.; Sun, J. Origin of the ductile-to-brittle transition of metastable β-titanium alloys: Self-hardening of ω-precipitates. *Acta Mater.* **2019**, *170*, 187–204. [CrossRef]
98. Fu, Y.; Xiao, W.; Wang, J.; Zhao, X.; Ma, C. Mechanical properties and deformation mechanisms of Ti-15Nb-5Zr-4Sn-1Fe alloy with varying α phase fraction. *J. Alloys Compd.* **2022**, *898*, 162816. [CrossRef]
99. Sun, F.; Zhang, J.Y.; Vermaut, P.; Choudhuri, D.; Alam, T.; Mantri, S.A.; Svec, P.; Gloriant, T.; Jacques, P.J.; Banerjee, R.; et al. Strengthening strategy for a ductile metastable β-titanium alloy using low-temperature aging. *Mater. Res. Lett.* **2017**, *5*, 547–553. [CrossRef]
100. Liu, H.; Niinomi, M.; Nakai, M.; Cho, K. Athermal and deformation-induced ω-phase transformations in biomedical beta-type alloy Ti-9Cr-0.2O. *Acta Mater.* **2016**, *106*, 162–170. [CrossRef]
101. Morinaga, M.; Yukawa, H.; Maya, T.; Sone, K.; Adachi, H. Theoretical design of titanium alloy. In Proceedings of the Sixth World Conference on Titanium. III, Cannes, France, 6−9 June 1998.
102. Ahmed, M.; Wexler, D.; Casillas, G.; Savvakin, D.G.; Pereloma, E.V. Strain rate dependence of deformation-induced transformation and twinning in a metastable titanium alloy. *Acta Mater.* **2016**, *104*, 190–200. [CrossRef]
103. Sadeghpour, S.; Abbasi, S.M.; Morakabati, M. Design of a New Multi-element Beta Titanium Alloy Based on d-Electron Method. In *TMS 2018 147th Annual Meeting & Exhibition Supplemental Proceedings*; The Minerals, Metals & Materials Series; Springer International Publishing: Cham, Switzerland, 2018; pp. 377–386.
104. Danard, Y.; Sun, F.; Gloriant, T.; Freiherr Von Thüngen, I.; Piellard, M.; Prima, F. The Influence of Twinning on the Strain–Hardenability in TRIP/TWIP Titanium Alloys: Role of Solute–Solution Strengthening. *Front. Mater.* **2020**, *7*, 240. [CrossRef]
105. Lilensten, L.; Danard, Y.; Brozek, C.; Mantri, S.; Castany, P.; Gloriant, T.; Vermaut, P.; Sun, F.; Banerjee, R.; Prima, F. On the heterogeneous nature of deformation in a strain-transformable beta metastable Ti-V-Cr-Al alloy. *Acta Mater.* **2019**, *162*, 268–276. [CrossRef]
106. Zhang, J.; Li, J.; Chen, G.; Liu, L.; Chen, Z.; Meng, Q.; Shen, B.; Sun, F.; Prima, F. Fabrication and characterization of a novel β metastable Ti-Mo-Zr alloy with large ductility and improved yield strength. *Mater. Charact.* **2018**, *139*, 421–427. [CrossRef]
107. Gordin, D.M.; Sun, F.; Laillé, D.; Prima, F.; Gloriant, T. How a new strain transformable titanium-based biomedical alloy can be designed for balloon expendable stents. *Materialia* **2020**, *10*, 100638. [CrossRef]
108. Wang, C.H.; Russell, A.M.; Cao, G.H. A semi-empirical approach to the prediction of deformation behaviors of β-Ti alloys. *Scr. Mater.* **2019**, *158*, 62–65. [CrossRef]
109. Bignon, M.; Bertrand, E.; Tancret, F.; Rivera-Díaz-del-Castillo, P.E.J. Modelling martensitic transformation in titanium alloys: The influence of temperature and deformation. *Materialia* **2019**, *7*, 100382. [CrossRef]
110. Mehjabeen, A.; Xu, W.; Qiu, D.; Qian, M. Redefining the β-Phase Stability in Ti-Nb-Zr Alloys for Alloy Design and Microstructural Prediction. *Jom-Us* **2018**, *70*, 2254–2259. [CrossRef]
111. Li, C.; Chen, J.H.; Wu, X.; Wang, W.; van der Zwaag, S. Tuning the stress induced martensitic formation in titanium alloys by alloy design. *J. Mater. Sci.* **2012**, *47*, 4093–4100. [CrossRef]
112. Kolli, R.P.; Joost, W.J.; Ankem, S. Phase Stability and Stress-Induced Transformations in Beta Titanium Alloys. *Jom-Us* **2015**, *67*, 1273–1280. [CrossRef]
113. Bania, P.J. Beta Titanium Alloys and Their Role in the Titanium Industry. *Jom-Us* **1994**, *46*, 16–19. [CrossRef]
114. Wang, Q.; Dong, C.; Liaw, P.K. Structural Stabilities of β-Ti Alloys Studied Using a New Mo Equivalent Derived from [β/(α + β)] Phase-Boundary Slopes. *Metall. Mater. Trans. A* **2015**, *46*, 3440–3447. [CrossRef]
115. Ikehata, H.; Nagasako, N.; Furuta, T.; Fukumoto, A.; Miwa, K.; Saito, T. First-principles calculations for development of low elastic modulus Ti alloys. *Phys. Rev. B* **2004**, *70*, 174113. [CrossRef]

116. Jawed, S.F.; Rabadia, C.D.; Liu, Y.J.; Wang, L.Q.; Li, Y.H.; Zhang, X.H.; Zhang, L.C. Beta-type Ti-Nb-Zr-Cr alloys with large plasticity and significant strain hardening. *Mater. Des.* **2019**, *181*, 108064. [CrossRef]
117. Jawed, S.F.; Rabadia, C.D.; Liu, Y.J.; Wang, L.Q.; Li, Y.H.; Zhang, X.H.; Zhang, L.C. Mechanical characterization and deformation behavior of β-stabilized Ti-Nb-Sn-Cr alloys. *J. Alloys Compd.* **2019**, *792*, 684–693. [CrossRef]
118. Wang, J.; Xiao, W.; Ren, L.; Fu, Y.; Ma, C. The roles of oxygen content on microstructural transformation, mechanical properties and corrosion resistance of Ti-Nb-based biomedical alloys with different β stabilities. *Mater. Charact.* **2021**, *176*, 111122. [CrossRef]
119. Abdel-Hady, M.; Fuwa, H.; Hinoshita, K.; Kimura, H.; Shinzato, Y.; Morinaga, M. Phase stability change with Zr content in β-type Ti-Nb alloys. *Scr. Mater.* **2007**, *57*, 1000–1003. [CrossRef]
120. Ijaz, M.F.; Kim, H.Y.; Hosoda, H.; Miyazaki, S. Effect of Sn addition on stress hysteresis and superelastic properties of a Ti-15Nb-3Mo alloy. *Scr. Mater.* **2014**, *72–73*, 29–32. [CrossRef]
121. Zou, C.; Li, J.; Wang, W.Y.; Zhang, Y.; Lin, D.; Yuan, R.; Wang, X.; Tang, B.; Wang, J.; Gao, X.; et al. Integrating data mining and machine learning to discover high-strength ductile titanium alloys. *Acta Mater.* **2021**, *202*, 211–221. [CrossRef]
122. Oh, J.M.; Narayana, P.L.; Hong, J.-K.; Yeom, J.-T.; Reddy, N.S.; Kang, N.; Park, C.H. Property optimization of TRIP Ti alloys based on artificial neural network. *J. Alloys Compd.* **2021**, *884*, 161029. [CrossRef]
123. Yang, F.; Li, Z.; Wang, Q.; Jiang, B.; Yan, B.; Zhang, P.; Xu, W.; Dong, C.; Liaw, P.K. Cluster-formula-embedded machine learning for design of multicomponent β-Ti alloys with low Young's modulus. *NPJ Comput. Mater.* **2020**, *6*, 101. [CrossRef]
124. Xu, Y.; Gao, J.; Huang, Y.; Rainforth, W.M. A low-cost metastable beta Ti alloy with high elastic admissible strain and enhanced ductility for orthopaedic application. *J. Alloys Compd.* **2020**, *835*, 155391. [CrossRef]
125. Li, Q.; Liu, T.; Li, J.; Cheng, C.; Niinomi, M.; Yamanaka, K.; Chiba, A.; Nakano, T. Microstructure, mechanical properties, and cytotoxicity of low Young's modulus Ti-Nb-Fe-Sn alloys. *J. Mater. Sci.* **2022**, *57*, 5634–5644. [CrossRef]
126. Min, X.; Bai, P.; Emura, S.; Ji, X.; Cheng, C.; Jiang, B.; Tsuchiya, K. Effect of oxygen content on deformation mode and corrosion behavior in β-type Ti-Mo alloy. *Mater. Sci. Eng. A* **2017**, *684*, 534–541. [CrossRef]
127. Wang, X.L.; Li, L.; Xing, H.; Ou, P.; Sun, J. Role of oxygen in stress-induced ω phase transformation and {3 3 2}<1 1 3> mechanical twinning in βTi-20V alloy. *Scr. Mater.* **2015**, *96*, 37–40. [CrossRef]
128. Ramarolahy, A.; Castany, P.; Prima, F.; Laheurte, P.; Peron, I.; Gloriant, T. Microstructure and mechanical behavior of superelastic Ti-24Nb-0.5O and Ti-24Nb-0.5N biomedical alloys. *J. Mech. Behav. Biomed. Mater.* **2012**, *9*, 83–90. [CrossRef] [PubMed]
129. Li, Q.; Ma, D.; Li, J.; Niinomi, M.; Nakai, M.; Koizumi, Y.; Wei, D.; Kakeshita, T.; Nakano, T.; Chiba, A.; et al. Low Young's Modulus Ti-Nb-O with High Strength and Good Plasticity. *Mater. Trans.* **2018**, *59*, 858–860. [CrossRef]
130. Zhang, B.; Huang, M.; Chong, Y.; Mao, W.; Gong, W.; Zheng, R.; Bai, Y.; Wang, D.; Sun, Q.; Wang, Y.; et al. Achieving large super-elasticity through changing relative easiness of deformation modes in Ti-Nb-Mo alloy by ultra-grain refinement. *Mater. Res. Lett.* **2021**, *9*, 223–230. [CrossRef]
131. Min, X.H.; Emura, S.; Tsuchiya, K.; Nishimura, T.; Tsuzaki, K. Transition of multi-deformation modes in Ti-10Mo alloy with oxygen addition. *Mater. Sci. Eng. A* **2014**, *590*, 88–96. [CrossRef]
132. Min, X.; Emura, S.; Zhang, L.; Tsuzaki, K.; Tsuchiya, K. Improvement of strength–ductility tradeoff in β titanium alloy through pre-strain induced twins combined with brittle ω phase. *Mater. Sci. Eng. A* **2015**, *646*, 279–287. [CrossRef]
133. Liu, H.; Niinomi, M.; Nakai, M.; Cho, K. β-Type titanium alloys for spinal fixation surgery with high Young's modulus variability and good mechanical properties. *Acta Biomater.* **2015**, *24*, 361–369. [CrossRef] [PubMed]
134. Qian, B.; Lilensten, L.; Zhang, J.; Yang, M.; Sun, F.; Vermaut, P.; Prima, F. On the transformation pathways in TRIP/TWIP Ti-12Mo alloy. *Mater. Sci. Eng. A* **2021**, *822*, 141672. [CrossRef]
135. Chong, Y.; Gholizadeh, R.; Guo, B.; Tsuru, T.; Zhao, G.; Yoshida, S.; Mitsuhara, M.; Godfrey, A.; Tsuji, N. Oxygen interstitials make metastable β titanium alloys strong and ductile. *Acta Mater.* **2023**, *257*, 119165. [CrossRef]
136. Liu, H.; Niinomi, M.; Nakai, M.; Cong, X.; Cho, K.; Boehlert, C.J.; Khademi, V. Abnormal Deformation Behavior of Oxygen-Modified β-Type Ti-29Nb-13Ta-4.6Zr Alloys for Biomedical Applications. *Metall. Mater. Trans. A* **2016**, *48*, 139–149. [CrossRef]
137. Chong, Y.; Gao, S.; Tsuji, N. A unique three-stage dependence of yielding behavior and strain-hardening ability in Ti-10V-2Fe-3Al alloy on phase fraction. *Mater. Sci. Eng. A* **2021**, *821*, 141609. [CrossRef]
138. Liao, Z.; Luan, B.; Zhang, X.; Liu, R.; Murty, K.L.; Liu, Q. Effect of varying α phase fraction on the mechanical properties and deformation mechanisms in a metastable β-ZrTiAlV alloy. *Mater. Sci. Eng. A* **2019**, *772*, 138784. [CrossRef]
139. Min, X.; Xiang, l.; Li, M.; Yao, K.; Emura, S.; Cheng, C.; Tsuchiya, K. Effect of {332}<113> Twins Combined with Isothermal w-Phase on Mechanical Properties in Ti-15Mo Alloy with Different Oxygen Contents. *Aata Metall. Sinica* **2018**, *54*, 1262–1272. [CrossRef]
140. Min, X.; Tsuzaki, K.; Emura, S.; Tsuchiya, K. Enhanced uniform elongation by pre-straining with deformation twinning in high-strength β-titanium alloys with an isothermal ω-phase. *Philos. Mag. Lett.* **2012**, *92*, 726–732. [CrossRef]
141. Church, N.L.; Hildyard, E.M.; Jones, N.G. The influence of grain size on the onset of the superelastic transformation in Ti-24Nb-4Sn-8Zr (wt%). *Mater. Sci. Eng. A* **2021**, *828*, 142072. [CrossRef]
142. Wang, J.; Xiao, W.; Fu, Y.; Ren, L.; Ma, C. Dependence of mechanical behavior on grain size of metastable Ti-Nb-O titanium alloy. *Prog. Nat. Sci. Mater. Inter.* **2022**, *32*, 63–71. [CrossRef]
143. Cai, M.-H.; Lee, C.-Y.; Lee, Y.-K. Effect of grain size on tensile properties of fine-grained metastable β titanium alloys fabricated by stress-induced martensite and its reverse transformations. *Scr. Mater.* **2012**, *66*, 606–609. [CrossRef]

144. Ma, X.; Chen, Z.; Xiao, L.; Lu, W.; Luo, S.; Mi, Y. Compressive deformation of a metastable β titanium alloy undergoing a stress-induced martensitic transformation: The role of β grain size. *Mater. Sci. Eng. A* **2020**, *794*, 139919. [CrossRef]
145. Bhattacharjee, A.; Bhargava, S.; Varma, V.K.; Kamat, S.V.; Gogia, A.K. Effect of b grain size on stress induced martensitic transformation in b solution treated Ti-10V-2Fe-3Al alloy. *Scr. Mater.* **2005**, *53*, 195–200. [CrossRef]
146. Xiao, J.F.; Shang, X.K.; Hou, J.H.; Li, Y.; He, B.B. Role of stress-induced martensite on damage behavior in a metastable titanium alloy. *Inter. J. Plast.* **2021**, *146*, 103103. [CrossRef]